

---

## Water Movements in lakes during Summer Stratification; Evidence from the Distribution of Temperature in Windermere

C. H. Mortimer

*Phil. Trans. R. Soc. Lond. B* 1952 **236**, 355-398  
doi: 10.1098/rstb.1952.0005

---

### Email alerting service

Receive free email alerts when new articles cite this article - sign up in the box at the top right-hand corner of the article or click [here](#)

---

To subscribe to *Phil. Trans. R. Soc. Lond. B* go to: <http://rstb.royalsocietypublishing.org/subscriptions>

---

WATER MOVEMENTS IN LAKES DURING SUMMER STRATIFICATION;  
EVIDENCE FROM THE DISTRIBUTION OF TEMPERATURE  
IN WINDERMERE

By C. H. MORTIMER, D.Sc.

*Freshwater Biological Association, The Ferry House, Ambleside, Westmorland*

WITH AN APPENDIX BY M. S. LONGUET-HIGGINS

*Trinity College, Cambridge*

*Communicated by W. H. Pearsall, F.R.S.—Received 24 May 1951—Revised 12 October 1951*

CONTENTS

	PAGE		PAGE
INTRODUCTION	356	A comparison of the internal wave pattern observed in Windermere with that computed for a three-layered basin	379
HISTORICAL REVIEW	357	Predicted flow in a three-layered model applied to Windermere	390
METHODS	360	Complicating factors in a lake	394
THE DISTRIBUTION OF TEMPERATURE IN THE NORTHERN BASIN OF WINDERMERE	364	The influence of internal waves on lake biology and sedimentation	394
DISCUSSION		SUMMARY	396
The universal nature of internal seiches	372	APPENDIX BY M. S. LONGUET-HIGGINS: OSCILLATIONS IN A THREE-LAYERED STRATIFIED BASIN	399
Flow in a two-layered basin	374	REFERENCES	402
Internal waves in a three-layered basin	375		
The response of a three-layered basin to wind stress	376		

The first part of this paper is taken up with an historical survey of the relatively few observations, some detailed and some less so, of internal seiches (internal standing waves) in lakes. After a description of the thermo-electric thermometer employed, there follow details and illustrations of the evidence, from temperature observations, for such internal waves in the northern basin of Windermere. Two main phases could be distinguished: (i) motion under wind stress leading to quasi-steady states with some or all of the isotherms tilted; (ii) internal seiche motion which developed after the wind had dropped. These observations confirm the findings of Wedderburn and his collaborators on the Scottish Lochs (1907–15). The results from Windermere are presented, not because any such confirmation is necessary, but in order to secure belated recognition of the fact that Wedderburn's 'temperature seiche' is not an isolated phenomenon, but is an everyday feature of movement in stratified lakes subject to wind action. As this movement is an important and largely unrecognized factor in lake environment, this paper is addressed mainly to limnologists. In its latter part, results of theoretical analyses of a detailed series of observations are presented in non-mathematical form. The applicability of a theory of oscillations in a basin with three layers of differing density (set out in an appendix by M. S. Longuet-Higgins) is tested by comparing theoretical and observed deflexions of selected isotherms from their equilibrium levels, resulting from internal waves after a gale. This theory also enables horizontal components of velocity and displacement to be calculated for each layer. Complicating factors in natural lakes are enumerated, and the influence of internal waves on lake biology and sedimentation is discussed.

## INTRODUCTION

Since Birge's (1916) paper it has been clearly recognized that the wind is an important, perhaps the most important, agent in producing the water movements which lead to mixing in lakes. Convection becomes important in surface layers during autumn and winter, but with that this paper will not deal.\* It is concerned with movements induced by wind, once summer thermal stratification has become established. In the absence of flow measurements, such movements in the northern basin of Windermere are inferred from changes in horizontal and vertical distribution of temperature. This approach to the problem is virtually one of necessity, for these movements rarely attain a velocity of more than a few centimetres per second, and instruments have yet to be devised to record adequately the distribution of such low velocities. But the *drift* of a water mass may be followed, if it can be suitably labelled, by drift bodies or drogues (Wasmund 1927-8; Mercanton 1932; Städler 1934), by chemical means or by any conservative property which serves to distinguish it from its surroundings. Over short time intervals, and within certain limits, heat content may be regarded as such a conservative property. The limits are set by heat exchange across the lake surface and exchange between the water masses themselves. In thermally stratified lakes, at least in those layers not immediately at the surface, the main picture of movement and mixing derived from studies of temperature distribution is not unduly blurred. The main reason for this is that the stability introduced by the vertical density gradient resists mixing, and any water layer which is separated from its neighbours by a temperature gradient of sufficient magnitude preserves a temporary identity.

For a more detailed description of summer thermal stratification and of the stages leading up to it the reader is referred to text-books (e.g. Welch 1935; Ruttner 1940). In essentials the lake is divided into a well-mixed, warm, surface layer, the *epilimnion*, which is separated from the colder and relatively stagnant bottom water, the *hypolimnion*, by an intermediate *metalimnion*. The upper part of this is usually characterized by a large vertical temperature gradient known as the *thermocline*. The depth of the epilimnion is an index of the extent to which wind energy can maintain mixing against the density gradient set up by warming from above (Munk & Anderson 1948). This is the framework within which movements take place. The effect of wind on flow in the epilimnion has been described by various workers, by inference in most cases, by measurement in a few (Wedderburn & Watson 1909; Wedderburn 1910; Hellström 1941). They agree that the main features are a rapid drift confined to the surface, and a slower return current in lower depths down to the thermocline. Flow below the thermocline is less understood, and hardly any reliable measurements have been made. We have only a number of opinions which are conflicting. Movement in the hypolimnion is nevertheless of considerable interest to the hydrobiologist, and has been the subject of detailed discussion by Hutchinson (1941) and the writer (Mortimer 1941, 1942, cf. pp. 170-178). In the latter study it was found that the transport of dissolved materials from the bottom mud into the overlying water layers could only be explained satisfactorily by a mechanism of turbulent diffusion resulting from flow which was mainly horizontal. Additional evidence was found

\* For recent views on convection see Montgomery *et al.* (1946).

to support the suggestion that a possible mechanism was provided by 'temperature seiches', occurring not as isolated events, but more or less continuously during summer stratification. The purpose of the present paper is to examine this suggestion, first in relation to previous work, and secondly in the light of events in Windermere. An attempt is made to interpret these events in the light of the theory of internal waves in model tanks with two and three layers of differing density. Addressed to hydrobiologists, this paper is in the main non-mathematical. An appendix on the theory of oscillations in a three-layered model is contributed by M. S. Longuet-Higgins.

#### HISTORICAL REVIEW

Rhythmic oscillations in the surface levels of lakes have long been known. Forel (1895, recognized them as uni- or multinodal standing waves, and introduced the term 'seiche' to hydrodynamics. Amplitudes of more than a few centimetres are only found on long lakes, and then only infrequently. In other cases special instruments are required to register the small amplitudes. When investigations of the vertical distribution of temperature became common, oscillations of much larger amplitude in the level of the isotherms were occasionally noticed. Thoulet (1894) could not explain the phenomenon, but called it 'une sorte de seiche interieure'. Richter (1897) found an approximately diurnal temperature cycle at 4 m depth in the Millstättersee.

The first correct interpretation of these oscillations was given by Watson (1904). He observed oscillations in the level of the thermocline in Loch Ness, with amplitudes of the order of 30 m and periods of 3 days. He interpreted them as standing waves on the interface between two fluids of differing density, and found fair agreement between the observed period and that calculated from equation (2), p. 359. More detailed observations by Wedderburn (1907, 1909, 1912), and Wedderburn & Young (1915), confirmed this interpretation, and united the observations with theory in an elegant manner. Wedderburn introduced the term 'temperature seiche', since commonly employed. The term 'internal seiche' is perhaps preferable, as this would also include cases, e.g. in the sea, in which density gradients depend on the distribution of solutes as well as temperature. Setting out originally to investigate the transfer of heat in the Wolfgangsee, Exner (1908*a, b*) found that his thermographs showed large oscillations in temperature at thermocline level with a period of nearly 24 h. He pointed out the similarity with Watson's findings, and this interpretation was confirmed by Schmidt (1908) in model experiments. Exner later (1928) also found good agreement between the period of thermocline oscillation in the Lunzer Untersee and that calculated from Watson's formula (2).

Watson (1904) and Schmidt (1908) made the simplifying assumption that the epilimnion and hypolimnion are both homogeneous, and that there is a sharp interface between them. A simplified diagram of the phases of inception and progress of an internal seiche is given as figure 1, with a rough indication of flow in the two layers. The seiche is a standing wave, set in motion by an initial displacement of the interface from the horizontal. In a natural lake this is effected by wind drag on the water surface (figure 1*a, b*). Surface epilimnion water is displaced toward the lee shore, where the thermocline becomes depressed below its equilibrium level. A corresponding rise in level of the isotherms occurs off the windward shore. This effect of wind in tilting the isotherms was originally demonstrated in several

Scottish fresh-water and sea lochs by Murray (1888). Theory demands, and observations confirm, that this tilt is maintained as long as the wind blows; indeed, the production of this tilt against gravity represents a large part of the work done by the wind. Although

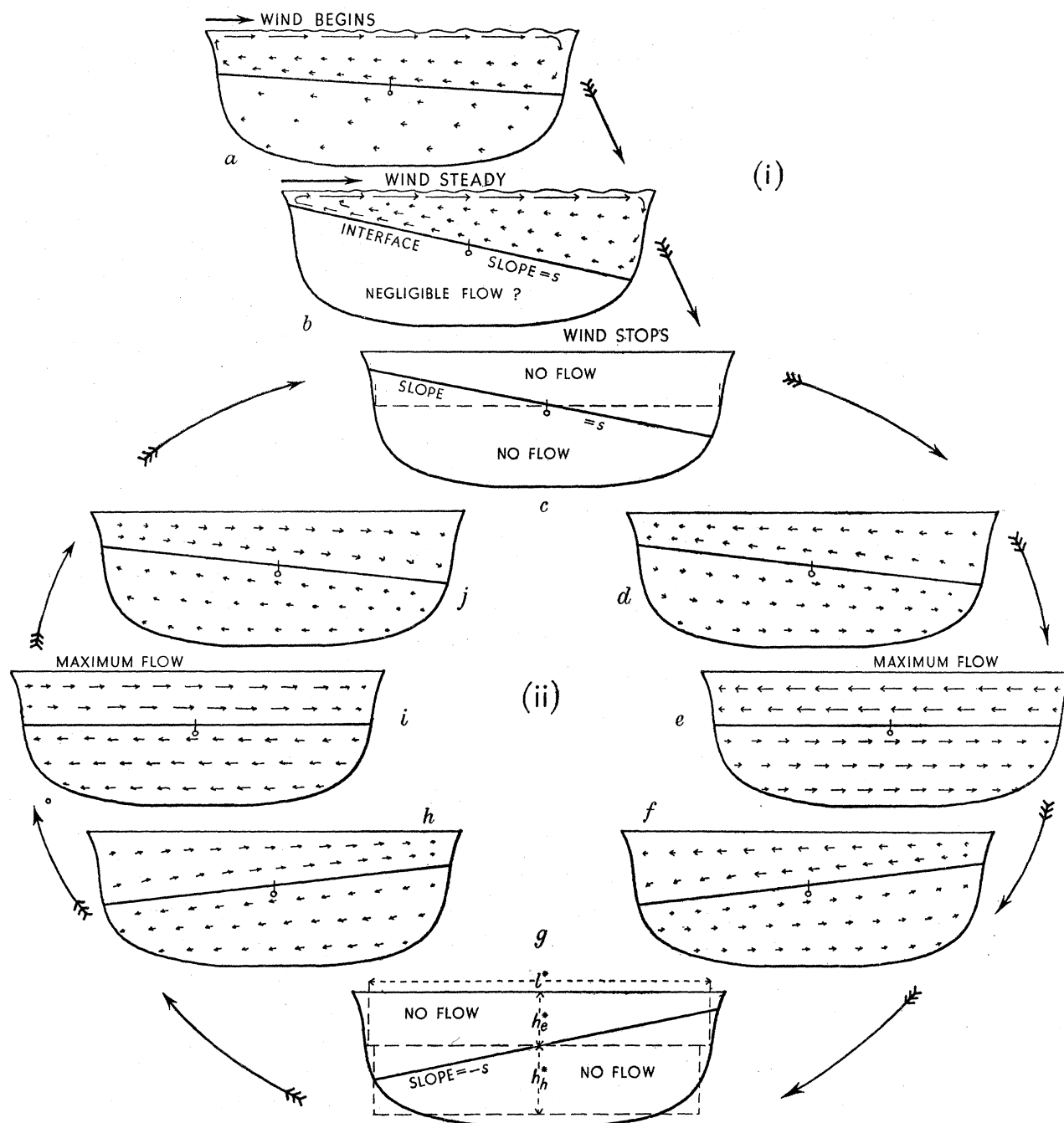


FIGURE 1. Movement caused by (i) wind stress and (ii) a subsequent internal seiche in a hypothetical two-layered lake, neglecting friction. Direction and velocity of flow are roughly indicated by arrows. \* refer to dimensions defined in the text.  $\odot$  = nodal section.

theoretical treatment of the effect of wind stress on stratified lakes is only in its very early stages (see later discussion), and although much more detailed observation and experiment is required to check theory, some results may be noted. If a steady wind blows across

a stratified lake consisting of an epilimnion of density  $\rho_e$  and a hypolimnion of density  $\rho_h$ , surface water is carried toward the leeward shore by frictional drag and wave action. This builds up a slope on the water surface, uphill in the direction of the wind, which causes a return flow in the lower part of the epilimnion. At the same time a much larger tilt appears at the interface, and is in the opposite sense to the tilt on the surface. The ratio of the surface slope to that of the interface will depend to some extent on the flow conditions which have become established, but the order of this ratio will be  $(\rho_h - \rho_e)/\rho_e$  (Hellström 1941). In natural lakes this is roughly 1/1000. Quite moderate winds are capable of maintaining a surface slope of 1 mm/km. We therefore may expect this to be accompanied by a thermocline slope of the order of 1 m/km. Thermocline slopes of this order are commonly observed (figures 7, 8 and 11; see also Wedderburn's papers). The important point is that, in order to produce such a thermocline slope, a comparatively large volume displacement of epi- and hypolimnion is required. Corresponding drifts with large horizontal components will therefore occur in both epi- and hypolimnion while a steady state is being built up in response to wind. This mainly horizontal shift of the two water masses will of course increase in scale as the density difference between epi- and hypolimnion diminishes, and the picture will be complicated by changing winds.

When the wind drops, the hydrostatic forces, which formerly helped to balance the wind drag, are now out of balance; they set up both surface and internal seiches with most of the energy concentrated in the latter. The slope on the water surface resolves into a surface seiche with a period, to a first approximation for the uninodal seiche, of

$$T = 2L/\sqrt{gD}, \quad (1)$$

where  $L$  is the length of the basin along the water surface,  $g$  is the acceleration due to gravity, and  $D$  the mean depth of the lake. Particularly fine examples are illustrated by Bergsten (1926). Similarly, the very much larger thermocline slope ( $s$  in figure 1) resolves into a series of oscillations of the type illustrated in figure 1, starting with a double amplitude of approximately  $sl$  (where  $l$  is the length along the interface), and continuing with decreasing amplitude until damped out by friction or, more usually, disturbed by further wind. This is the type of oscillation treated in papers already quoted, and of those described in this paper. It has a period which is very much longer than that of the surface seiche. For the simplified case of a rectangular lake of length  $l$  much greater than depth, and with a homogeneous epi- and hypolimnion of thickness  $h_e$  and  $h_h$  and density  $\rho_e$  and  $\rho_h$  respectively, the period of the uninodal internal seiche is given by:

$$T = \frac{2l}{\sqrt{\left\{g(\rho_h - \rho_e) \left/ \left( \frac{\rho_h}{h_h} + \frac{\rho_e}{h_e} \right) \right\}}}. \quad (2)$$

This is the formula used by Watson (1904) and Schmidt (1908), and will be later referred to as Watson's formula, although it was derived much earlier. A better approximation to conditions in natural lakes can be made by applying more complex theory which takes the shape of the basin into account (Wedderburn 1911; Proudman 1914; Aichi 1918; Defant 1918); but a complete theory which includes friction and the rotation of the earth has yet to be produced.

The great achievement of Wedderburn and his collaborators was the illustration, in considerable detail, of the course of the isotherms during these oscillations, and the way in which they were affected by wind. Less success attended their efforts to measure the currents. The velocities were near, or below, the lower sensitivity limit of the instruments employed, and the results, for the hypolimnion at least, were inconclusive. However, the main features of flow due to the seiche alone were predicted for an idealized lake by Wedderburn & Williams (1911), and are indicated in figure 1. Except at the ends of the basin, where vertical components of flow become important, the seiche is characterized by a horizontal drift, which changes sign at each half-cycle and is opposite in phase in the epi- and hypolimnion. Wedderburn's current measurements generally confirmed this picture, although his observations (1912, p. 633) suggest that 'currents in the lochs are not so simple as has been supposed, and that there is considerable scope for their investigation'.

Even less is known of the flow distribution when the wind is still blowing, and we may expect a fairly complex series of events (cf. Johnsson 1946, 1948) before the steady state illustrated in figure 1*b* is set up. Further discussion of flow, together with speculation on why limnologists in general have failed to apply Wedderburn's findings, is deferred to a later section.

#### METHODS

For rapid exploration of temperature distribution in the lake, a thermo-electric thermometer was used, similar to that described by Saunders & Ulliyott (1937). Thirty copper-constantan couples were arranged in series, with one set of junctions projecting into the water, and the other set maintained at a known temperature in a Thermos flask, inside a protective casing. In Saunders's instrument, the Thermos flask was pressure-protected and filled with crushed ice; in the present instrument, it was arranged to fill the Thermos flask with surface water, the temperature of which was measured with a mercury thermometer. This procedure was first successfully adopted by Gilson (unpublished communication) in an instrument used on the Percy Sladen Trust Expedition to Lake Titicaca in 1937. The temperature change inside the Thermos flask, during the time required for one vertical series of measurements, was found to be negligible.

The instrument is illustrated in figure 2. It consisted of a base-ring, *B*, carrying a framework which supported a can, *C*, which housed a Thermos flask. Both the can and its Thermos flask were mounted mouth downwards, and the can was provided with a lid, *L*, which slid on the framework, and was spring-loaded to close. The lid carried the thermocouple assembly and a bung, arranged so that the Thermos flask was sealed from the rest of the can when the lid was closed. Both can and Thermos flask were filled with surface water by holding the apparatus upside down a few inches under water, with the lid held open by the handles, *H*. After closing, the instrument was allowed to swing right side up, while still under water, and raised until the external junctions, *E*, were just below the surface. With the Thermos flask sealed off in this way, and surrounded by surface water in the can, adequate thermal insulation was provided for the internal junctions, *I*.

If the temperature of Thermos flask and container were initially widely different from that of the surface water, it was necessary to empty and re-fill once or twice until zero current on the galvanometer indicated that inside and outside temperatures were the same, but this usually took less than a minute. The temperature of the water near the external

junctions was then measured to the nearest  $\frac{1}{20}^{\circ}$  C with a mercury thermometer with the bulb suitably shaded. A built-in thermometer would have been an improvement, but this was ruled out by the evolution of the instrument, which started with a series of concentric baffles as a thermal insulator, later found to be inadequate.

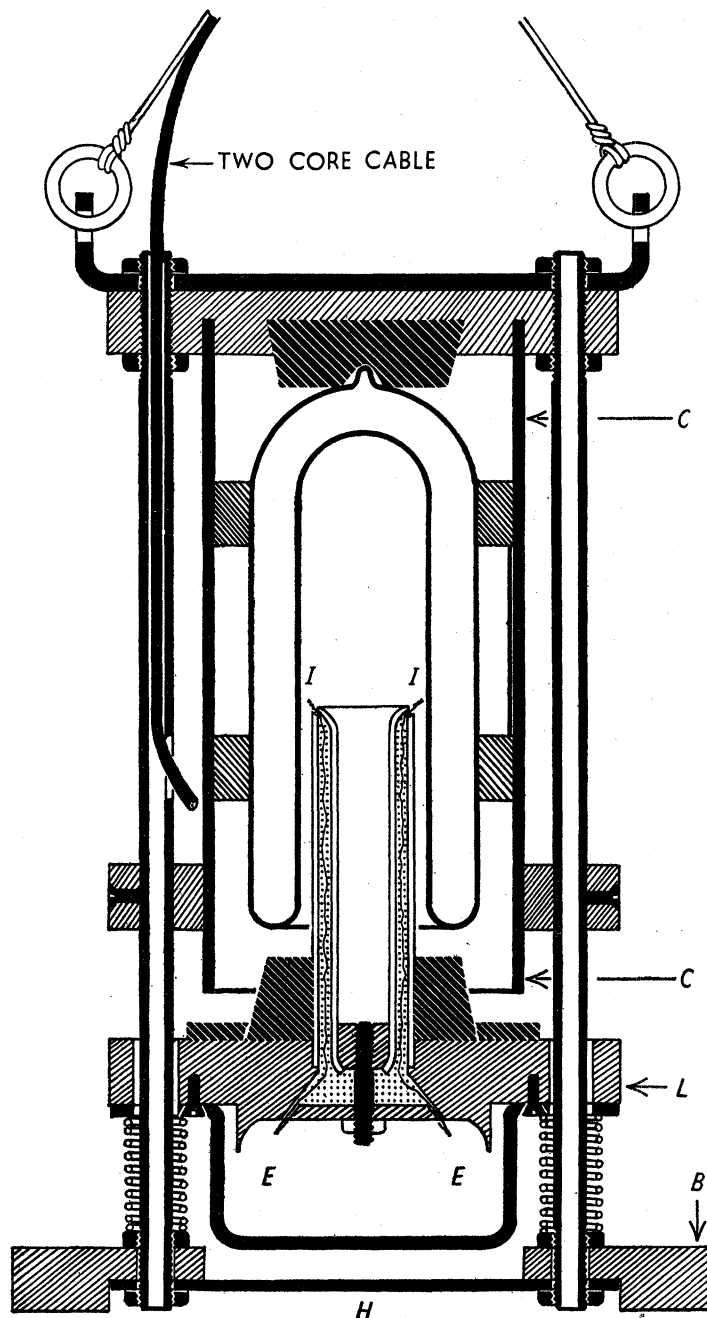


FIGURE 2. Thermo-electric thermometer.

With the boat anchored, the instrument was lowered by its two-cored electric cable from a suitable winch over a depth-measuring sheave. Differences between the external temperature and that inside the instrument produced a corresponding thermo-current through a Cambridge Unipivot galvanometer of low resistance as used by Saunders & Ulliyott (1937).



Their precautions in design were observed and the equipment was calibrated at known temperatures in the laboratory.

It was possible to obtain a sufficiently detailed picture of temperature distribution at any one station in about 10 min. Galvanometer readings, the more closely spaced in depth the greater the temperature gradient, were later converted into temperature to the nearest

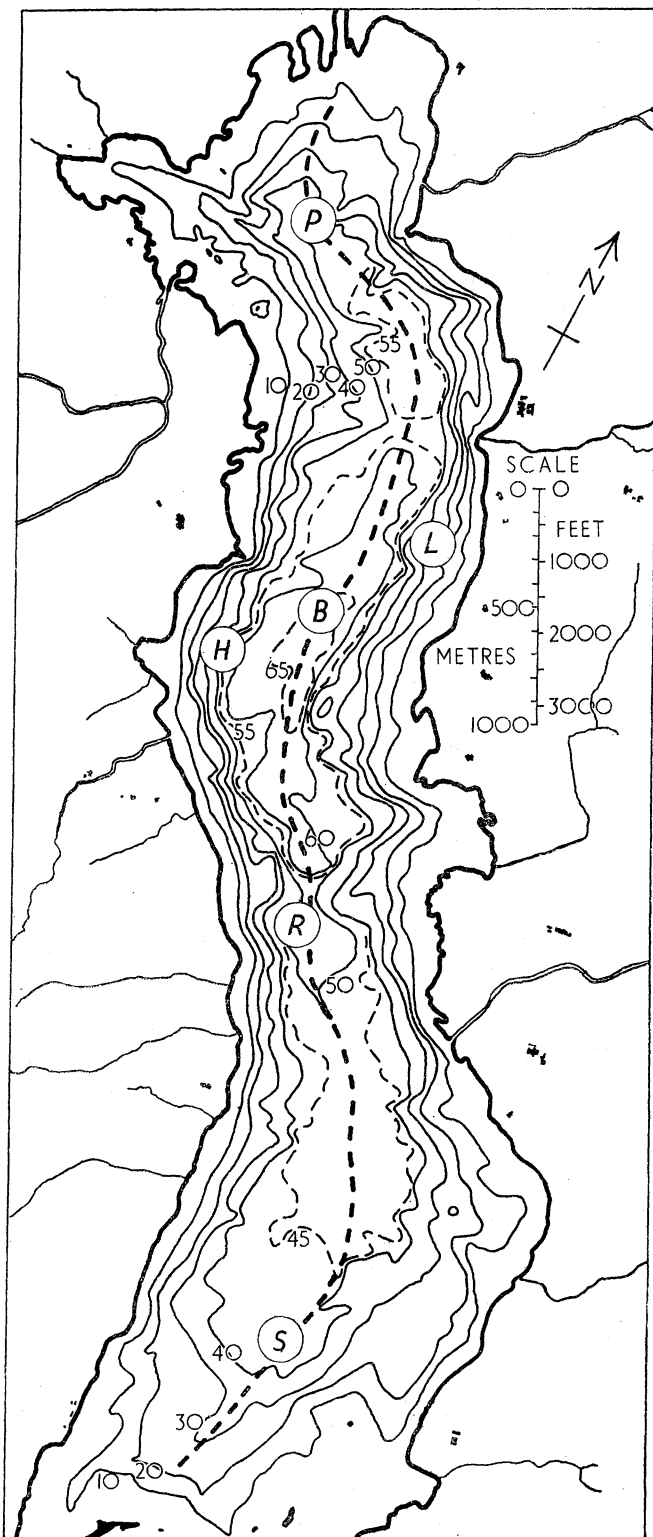


FIGURE 3. Chart of Windermere northern basin, based on the 1937 Admiralty echosounding survey. Depth contours in metres. The measuring stations are indicated by letters, and the approximate medial track by a thick broken line.

0.05° C, which was considered to be the limit of accuracy of the instrument in the field. These readings were then entered at the appropriate depths in section diagrams (see later figures), and the isotherms interpolated by inspection.

The great advantage of electrical thermometers for this type of work lies in their speed of operation. It is of interest that this was also noted by the first users of thermocouples for the exploration of lake temperature (Becquerel & Breschet 1836) on the Lake of Geneva. On Windermere it was possible to cover up to eight stations within 2 hours and obtain a reasonably synoptic picture of temperature distribution. To achieve this by classical methods would require a multitude of observers and reversing thermometers. Wedderburn and his party probably reached the practical limit of that method. In passing it may be noted that the bathythermograph (Spilhaus 1938) may also be used for rapid surveys, and possesses the great advantage that measurements can be made from a moving boat. The loss in accuracy compared with the instrument described here could be tolerated for many purposes, but in comparative tests\* it was found that the time saved in the field was more than offset by that required later in handling and reading the bathythermograph records. If the bathythermograph is used from a boat under way there is some lack of precision in position of the station, which may cause serious error on a small lake. Electrometric techniques have the advantage in giving the information in convenient form for immediate plotting, especially if the instrument is set to each isotherm in turn and lowered to the appropriate depth; but for accurate work it is essential that the cable is vertical. In practice this usually requires anchoring, and for greater speed of working moorings were set out on all stations (figure 3).

Figure 3 is a chart of the northern basin of Windermere with depth contours taken from the 1937 Admiralty survey, showing the position of stations worked. Four stations were placed as far as possible along the 'deep track', i.e. a smoothed medial line drawn through the deepest points on the Admiralty survey cross-sections, which were spaced at approximately 60-yard intervals. In the absence of any regular axis, this track was taken as the longitudinal section.

It is unfortunate that wind recordings were not available for any of the periods under review. However, for this largely descriptive study, rough estimates suffice. These are entered in figures and text as Beaufort numbers with direction and occasional notes of previous wind conditions. For instance, 'WNW 5 to 6, 12 h' means that a wind of that approximate force and direction had been blowing for about 12 h previously. On Windermere it is difficult to get a reliable estimate of wind, especially if it has a large westerly component. Varying shelter along the west shore considerably affects the force and direction in different parts of the basin. Wherever possible, simpler conditions were selected for study, i.e. relatively steady winds blowing nearly up or down the lake.

An under-water thermograph designed and used by Wedderburn & Young (1915) was put into operation for one series of measurements. Results are given in figure 12.

\* I am indebted to Dr J. N. Carruthers of the Admiralty Hydrographic Department for the opportunity to carry out these tests.

## THE DISTRIBUTION OF TEMPERATURE IN THE NORTHERN BASIN OF WINDERMERE

The starting point for this investigation occurred in May 1947 when measurements of the vertical distribution of temperature were being made at station *B* as a background for other work. This station, although not exactly central, is near the deepest point, and had been used as the routine sampling station for the northern basin. After an exceptionally cold winter with partial ice cover, the lake remained homothermal while warming up to nearly 6° C at the end of April. By the end of May it had become sharply stratified with the surface water at 14° C (figure 4). At this stage it became clear that events could not be

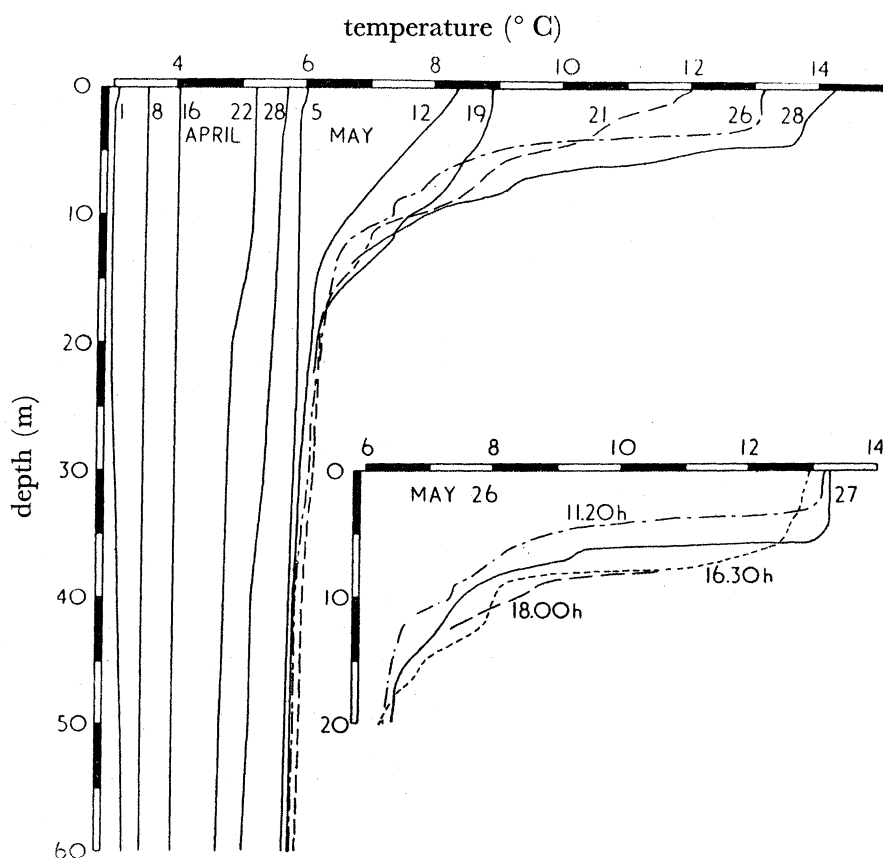


FIGURE 4. Vertical distribution of temperature at station *B*, Windermere northern basin, at approximately weekly intervals from 1 January to 19 May 1947, thereafter more frequently until 28 May, and on three occasions on 26 May 1947.

explained by purely vertical heat exchange in the water column, but that large-scale horizontal transfer was taking place. This is illustrated by the comparison in figure 4 between the temperature of the layer between 5 and 20 m on the two dates 21 and 26 May and, more strikingly, between 11.20 h and 16.30 h on the latter date. During that morning a south-south-east wind of force 6 began to blow up the lake, and it seemed reasonable to conclude that this had transported epilimnion water northwards and caused the depression of the thermocline observed 5 h later at *B*. This view was confirmed on the next occasion of a southerly wind, when measurements were made on a longitudinal section (figure 5). The original surface water, above 14° C, had been transported to the north end of the

lake, and the  $12^{\circ}$  C isotherm lay at 7.7 m at *P* and at 2.5 m at *S* with a slope of 1.2 m/km between *P* and *R*. After an intervening calm spell, the water warmer than  $14^{\circ}$  had flowed back beyond *R*, and the thermocline showed a slight slope in the opposite direction. This reversal may be regarded as the beginning of a temperature seiche, and measurements

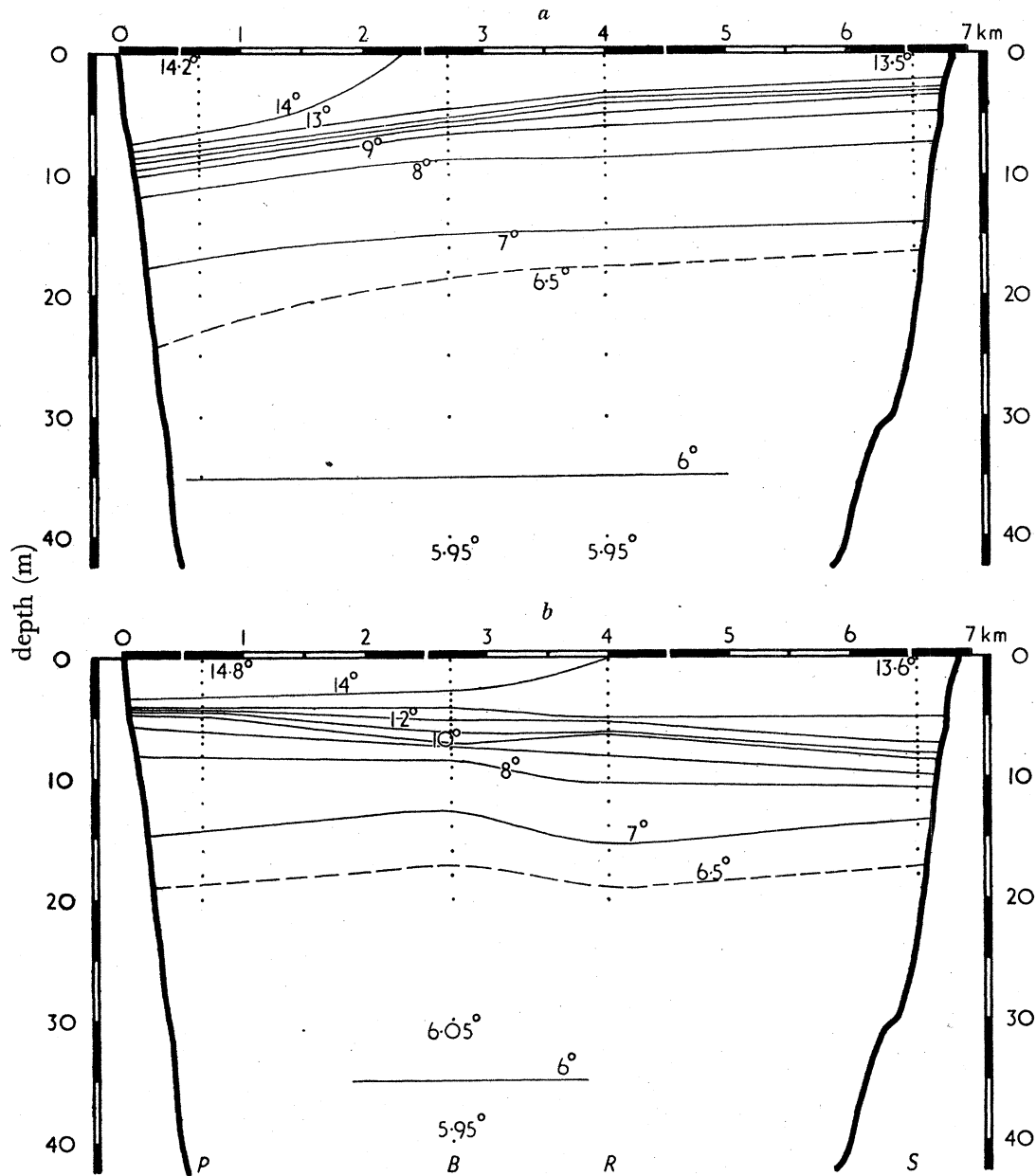


FIGURE 5. Distribution of temperature in a longitudinal section of Windermere northern basin, (a) on 28 May 1947 (15.10 to 17.07 h) after an east-south-east wind had been blowing at force 6 for about 4 h, and (b) on 29 May 1947 (09.07 to 10.58 h) after a calm night. Letters indicate measuring stations. The vertical scale is  $100 \times$  the horizontal.

continued at *B* at daily or more frequent intervals from 26 May until 21 June (figure 6) show continual fluctuations in level of the thermocline, especially during and after windy spells. It is also significant that, in figure 6, the more closely spaced the observations are in time, the greater these fluctuations appear to be.

Figure 5 illustrates a longitudinal tilt of the isotherms by a moderate wind blowing more or less up the lake. A cross-wind also resulted in a corresponding transverse displacement on the cross-section *HBL*, illustrated in figure 7. Here the southerly wind of 26 May had veered during that afternoon to south-west and had blown from that quarter at force 5 to 6 for 24 h, to produce the thermocline ( $12^{\circ}$  isotherm) slope of 4 m/km shown in the figure. Eighteen hours later, after a night's comparative calm, the isotherms had swung back to a more or less level position. As station *B* is common to both this and the longitudinal section, it is clear that, with changing winds, the structure of the water column at *B* is subject to influences of considerable complexity.

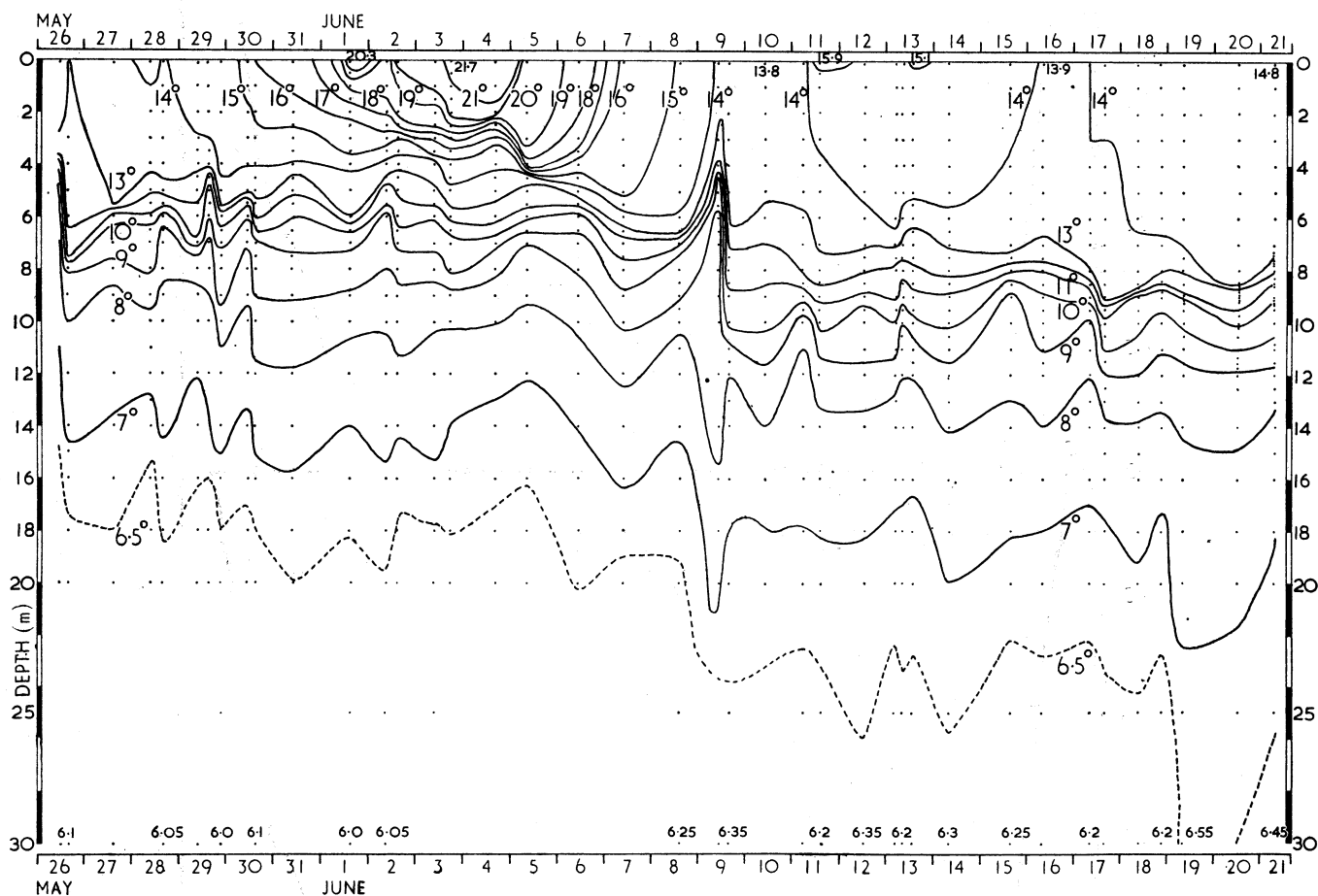


FIGURE 6. Changes in distribution of temperature at station *B*, Windermere northern basin, from 26 May to 21 June 1947.

On 9 June a north-westerly gale of force 7 to 8, preceded by strong west to north-west winds, was followed by 5 days' calm. This afforded an excellent opportunity for observing the two main phases of movement clearly separated. These were, first, a displacement of the isotherms by the wind and, secondly, internal seiches which followed when the wind had dropped. The hot calm spell of 29 May to 3 June had produced the conditions in the surface layers, illustrated in figures 6 and 21, the temperature being above  $21^{\circ}$  C at the surface and decreasing more or less regularly with depth at a rate of about  $1.6^{\circ}/\text{m}$  to  $11^{\circ}$  C at 6.5 m, with no well-marked thermocline. This typical calm weather condition was then disturbed by unsettled squally winds, mainly from the north-west, during the period

5 to 8 June, with the result that on the latter date the top 5 m were uniformly mixed at  $14.7^{\circ}\text{C}$ , and there was a sharp thermocline with a  $4^{\circ}$  drop between 6 and 8 m. Inspection of figure 6 shows that this transition to a typically windy weather condition had taken place without any large change in the mean temperature of the top 19 m ( $13.5^{\circ}\text{C}$  on 3 June,  $13.7^{\circ}\text{C}$  on 7 June).

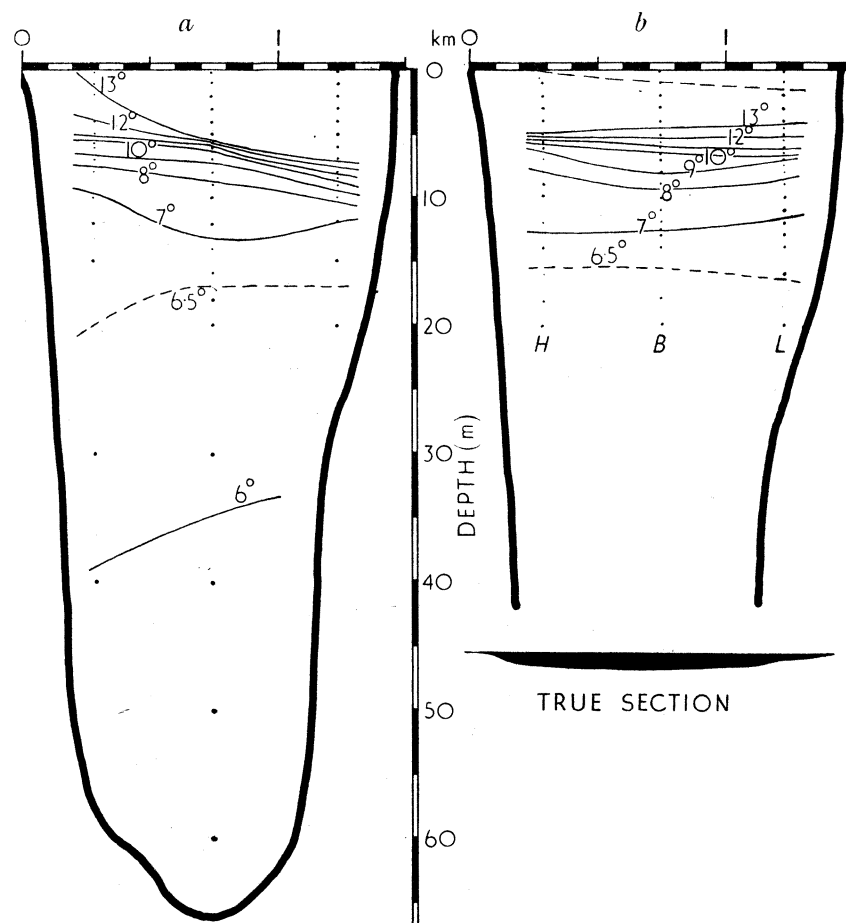


FIGURE 7. Distribution of temperature in a cross-section of Windermere northern basin, (a) on 27 May 1947 (15.00 to 16.30 h) after a south-westerly wind had been blowing at force 5 to 6 for a day, and (b) on 28 May 1947 (10.20 to 11.22 h) after 18 h calm. Letters indicate measuring stations. Vertical scale is  $50\times$  the horizontal. The black silhouette represents the section in true proportions.

It is not immediately apparent why the large mixing forces operating during windy weather serve to preserve, and even accentuate, the thermocline rather than destroy it. Figure 8*b* provides part of the answer. This figure shows the position of the isotherms after a period of strong north-west winds had culminated on 9 June in a moderate north-north-west gale (force 7 to 8) blowing almost straight down the lake. All the surface water above  $14^{\circ}\text{C}$  had been dragged to the leeward half of the lake, and the thermocline at this end was very sharp ( $4^{\circ}/\text{m}$  at *S*). At the windward end conditions were very different. Most of the metalimnion (here defined as the transitional layer between the steepest temperature gradient, the thermocline, and that lower part of the hypolimnion which is nearly isothermal) had been shifted to the windward half. The isotherms were curved upward and

cut the surface at widely spaced intervals from  $14^{\circ}$  at a mid-lake position to  $7^{\circ}$  at the windward end. Table 1 gives further proof that the water, at that time lying at the surface at the windward end, was in fact hypolimnion water which had welled up to replace the original epilimnion totally removed by the wind. While it is not the purpose of this paper to discuss this phenomenon in detail, it may be pointed out that when bottom and intermediate water has been forced to the surface it will become incorporated in the rapid surface drift, if the wind continues long enough, and so mix into the epilimnion, which will consequently

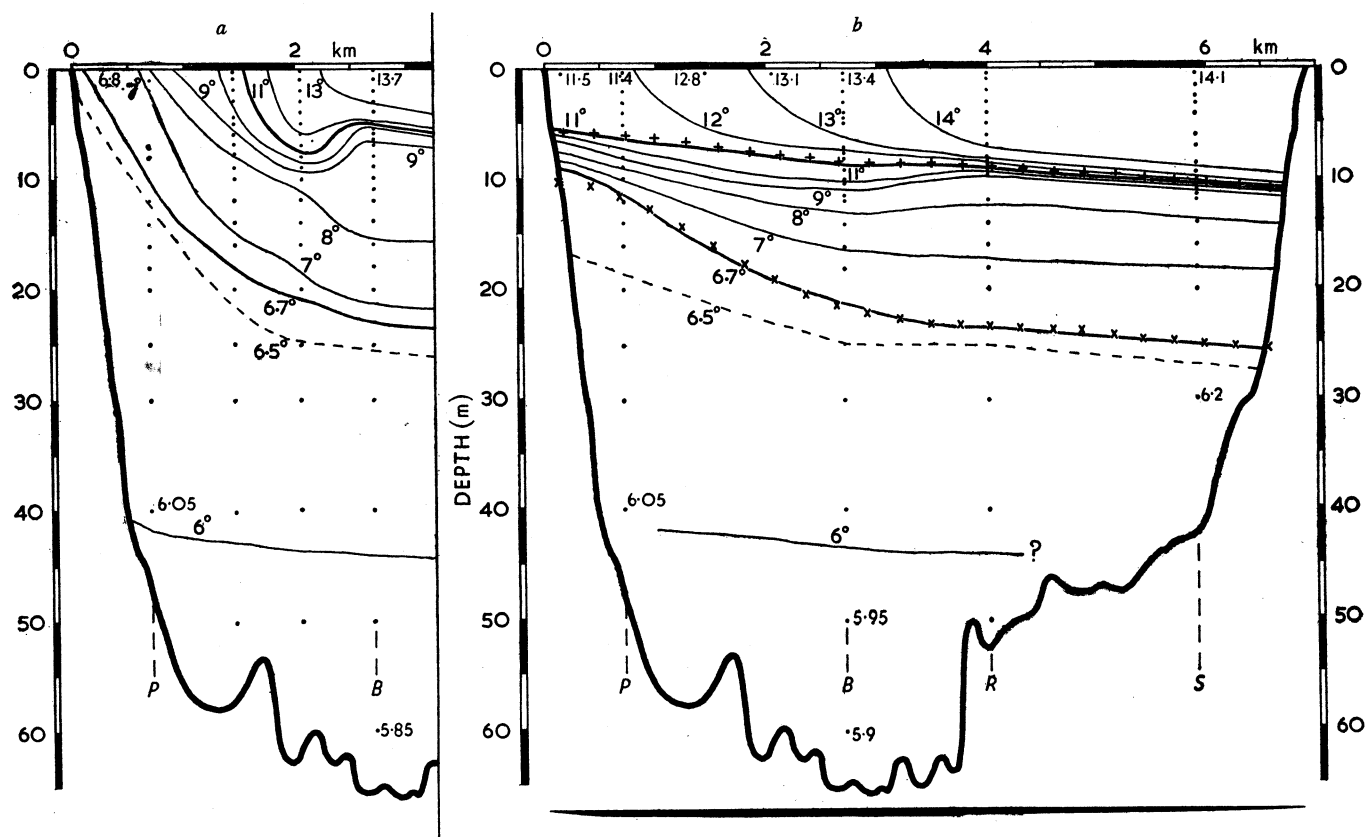


FIGURE 8. Distribution of temperature in a longitudinal section of Windermere northern basin on 9 June 1947, (a) during the morning (10.30 to 12.10 h) at the height of a north-westerly gale of force 7 to 8, and (b) during the afternoon (15.25 to 17.14) as the gale was moderating. Letters indicate measuring stations. The vertical scale is  $100 \times$  the horizontal. The black silhouette at the base of (b) represents the section in true proportions. The crosses in (b) indicate cosine series fitted to the  $11^{\circ}$  and  $6.7^{\circ}$  isotherms as follows (further details on p. 386):

$$11^{\circ} (+ +) = 8.5 - (2.08 \cos \pi x/l + 0.28 \cos 2\pi x/l + 0.46 \cos 3\pi x/l) \text{ metres depth;}$$

$$6.7^{\circ} (\times \times) = 20.5 - (6.40 \cos \pi x/l + 2.62 \cos 2\pi x/l + 1.33 \cos 3\pi x/l) \text{ metres depth.}$$

decrease in temperature and increase in depth. Removal of intermediate water into the new epilimnion is a mechanism which may help to explain the steepening of the thermocline commonly observed after moderate winds have been blowing for some time. Experiments mentioned later (figure 14) suggest that violent winds of short duration can have a very different effect.

By the morning of 10 June the wind had dropped; the position of the isotherms on a longitudinal section at this time is shown in figure 9. Apart from occasional light breezes, calm conditions persisted for several days. This opportunity was taken to follow the course

## WATER MOVEMENTS IN LAKES

369

of the internal seiche in detail at station *P*, near the northern antinode of the uninodal seiche. Hourly observations of the vertical distribution of temperature over a period of 76 h are presented in a depth-time diagram (figure 10). The main feature is a fairly regular oscillation at thermocline level (indicated by a thickened line for the 11° isotherm) of

TABLE 1.\* COMPARISON OF SURFACE WATER AT STATION *P*, 9 JUNE 1947, WITH WATER FROM DIFFERENT DEPTHS AT STATION *B* ON THE SAME DATE

station and depth (m)	temp. (° C)	alkalinity (mg/l. CaCO <sub>3</sub> )	silicate (mg/l. SiO <sub>2</sub> )	<i>Asterionella formosa</i> Hass.	
				numbers of living cells per mm <sup>3</sup> (to 5% confidence limits)	mean number of cells per colony
<i>P</i> 0	7.8	6.85	2.2	0.49-0.66	3.6
<i>B</i> 0	13.7	7.9	0.45	3.2-5.1	8.9
10	10.8	7.1	1.55	1.8-2.5	5.2
20	6.7	7.0	2.0	0.61-0.84	3.2
30	6.35	6.8	2.0	0.37-0.47	3.2

\* I am indebted to Miss B. Knudson and Mr F. J. Mackereth for the data in this table.

amplitude 2 to 3 m and period 18 to 19 h. This period is in good agreement with that calculated for a uninodal seiche from Watson's formula. If we assume that we are dealing with two layers only, and insert reasonable mean values (see table 2),  $l=6.6$  km,  $h_e=7.0$  m,  $h_h=28$  m, and  $(\rho_h-\rho_e)=7.05 \times 10^{-4}$ , we obtain  $T=18.8$  h.

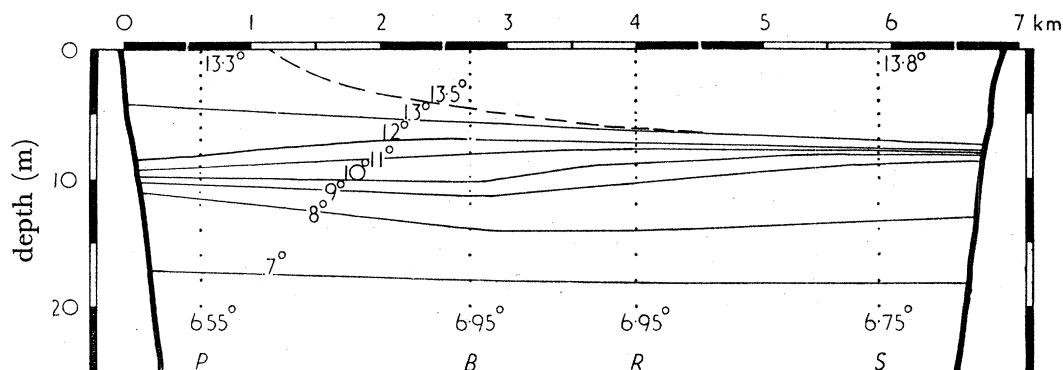
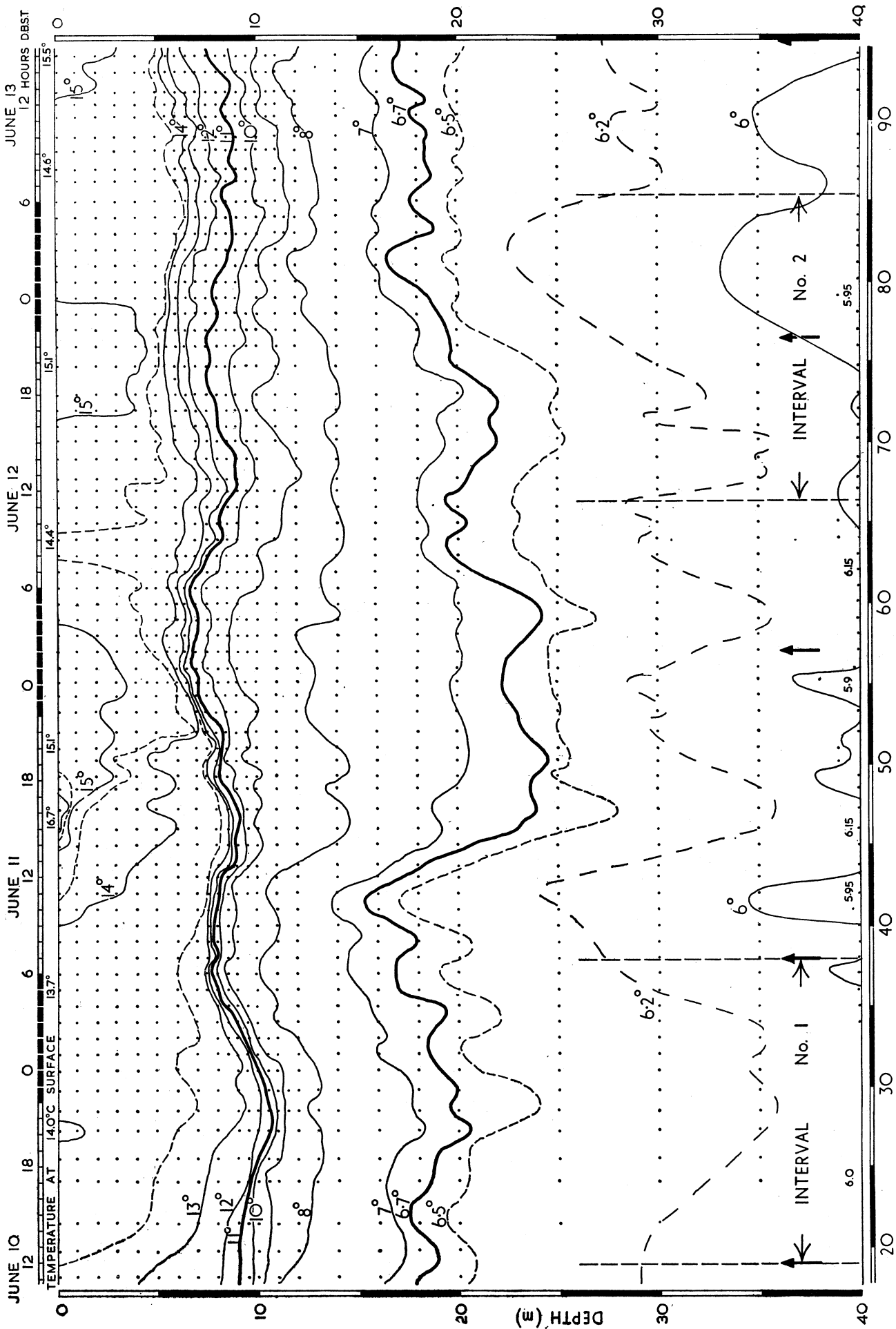


FIGURE 9. Distribution of temperature in a longitudinal section of Windermere northern basin on 10 June 1947 (09.10 to 11.10 h), calm since previous evening. Letters indicate measuring stations. The vertical scale is  $100 \times$  the horizontal.

Initially the thermocline was sharp, but it became progressively less so as the oscillation proceeded, owing presumably to the mixing produced by shear between epi- and hypolimnion. Damping of the main oscillation became noticeable after the second complete cycle, and there was a definite, but so far unexplained, gradual rise in level of the thermocline during the first two cycles. Superimposed on the main wave were oscillations of much shorter period, 2 to 3 h. Their origin can only be surmised. They may have been transverse oscillations, progressive internal waves (see p. 394) or perhaps a seiche in Pullwyke Bay. The movement of the lower isotherms (e.g. 7°), which was considerable, was not in phase with that at the thermocline level, pointing to other internal waves of much longer period





scale in hours to fit figures 19 and 22

FIGURE 10. Changes in vertical temperature distribution at station P, Windermere northern basin, from 11.00 h 10 June to 15.00 h 13 June 1947. The arrows and interval limits will be referred to in the text.

at sub-thermocline levels. These are the subject of later discussion. Oscillations in sub-thermocline layers may be expected in natural lakes and, because of the small density gradients at these levels, such internal waves will be of much longer period, and possibly larger amplitude, than the oscillation at thermocline level. The movement of deep water of temperature below  $6^{\circ}\text{C}$  into and out of the lower part of the section (figure 10) may be regarded as the result of such a long-period oscillation. With the very small density gradient in this region, the amplitude of movement of the  $6^{\circ}$  isotherm was large.

Another feature worthy of note is the effect of diurnal heating and nocturnal cooling in the surface layers. 11 June provides an example of an exceptionally hot, calm day which had produced high temperatures at the surface by the afternoon. Cooling and convection during the following night had mixed the epilimnion almost completely by morning.

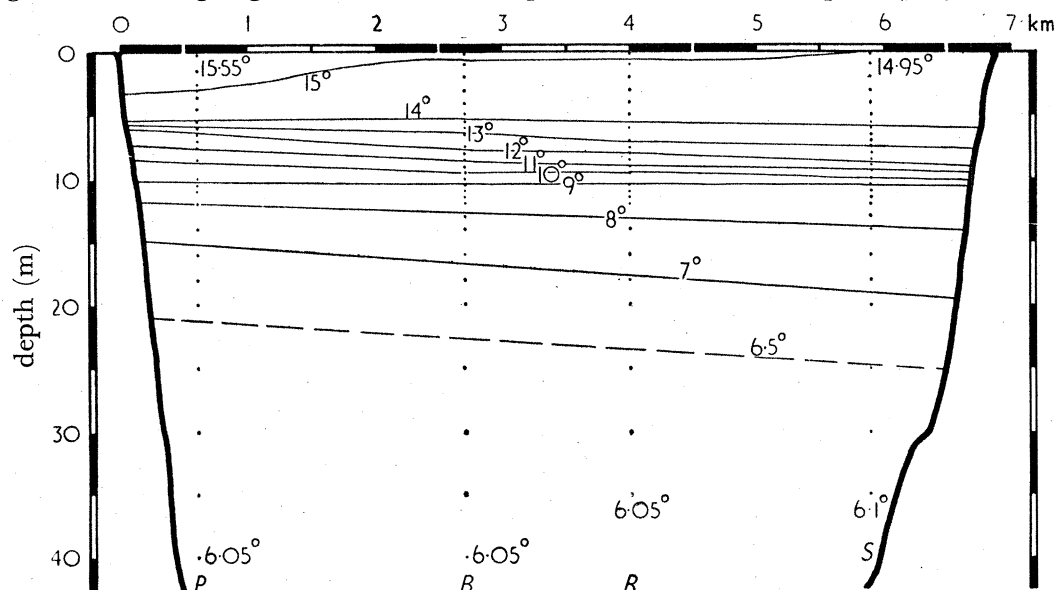


FIGURE 11. Distribution of temperature in a longitudinal section of Windermere northern basin on 13 June (15.00 to 16.57 h), calm since 10 June. Letters indicate measuring stations. The vertical scale is  $100 \times$  the horizontal.

Figure 11 illustrates a longitudinal series taken immediately on completion of the hourly observations at station *P*. Subsequent but less detailed observations, not illustrated, show that the oscillation which started on 9 June continued with decreasing amplitude until disturbed by a north-west wind on 15 June. Spells of southerly wind during the next 2 days were so timed that they built up an oscillation of large amplitude with a period of about 17 h, which continued until again disturbed by wind on 20 June.

The general conclusion is that quite moderate winds can set the water masses in motion, and that motion continues in the form of internal waves during the intervening calm spells. This is further illustrated by figure 12, which is a thermograph record at 9.5 m depth at station *P* from 24 June to 4 July. The thermograph used was the one described by Wedderburn & Young (1915), and was kindly lent by the Royal Scottish Museum. The instrument was calibrated before and after this series, and occasional measurements of vertical temperature distribution at *P* provided additional checks; these are indicated by dots in the figure. Rough estimates of wind are indicated by length and direction of arrows, north being at the top of the diagram. A rising arrow, i.e. a wind with a large southerly

component, may be expected to cause a displacement which will raise the temperature at the thermograph, and wind with a northerly component will have the opposite effect. Cross-winds might be relatively ineffective. The shape and amplitude of the record were determined not only by features of the oscillation but depended also on the position of the thermograph in relation to the mean level of the thermocline; a simple two-layered system would of course produce a square-topped wave. In spite of the fact that the record was confined to one depth, it shows that the water was never at rest. Displacements forced

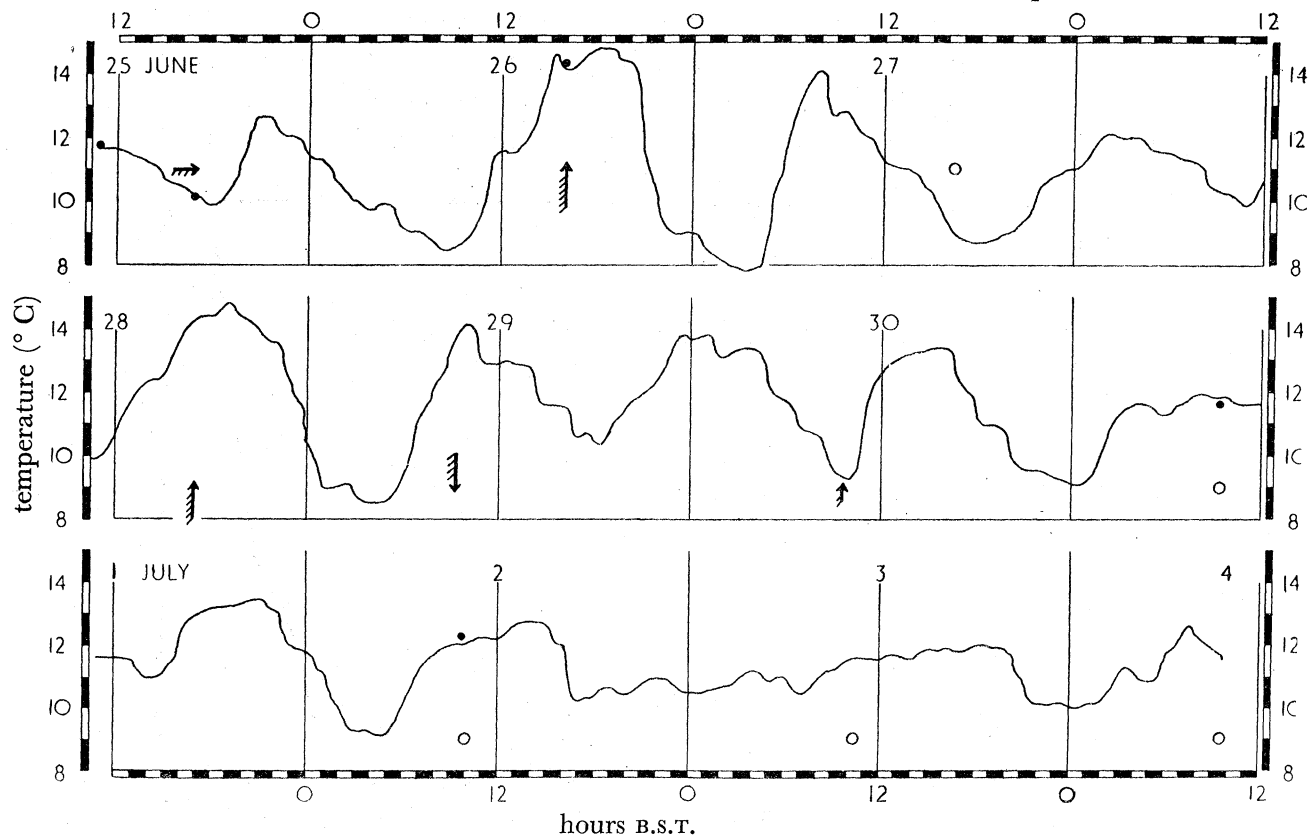


FIGURE 12. A continuous record of temperature at 9.5 m depth at station *P*, Windermere northern basin, from 25 June to 4 July 1947. Approximate wind direction and force is indicated by arrows, no wind is shown by circles, and temperature checks by dots (for details consult text).

by the wind were evident on 26 and 28 June, and there was some indication of damping by wind on the 29th. An oscillation with a period of 14 to 15 h continued during the calm spell after the 29th, but with apparently decreasing amplitude. Again, 'wavelets' of 2 to 3 h period are indicated (cf. figure 10), although interpretation is difficult with a record of this kind, which depends not only on movement, but also on the vertical structure of the thermocline.

#### DISCUSSION

##### *The universal nature of internal seiches*

From the foregoing survey of previous work and from the findings in Windermere it is apparent that, wherever a lake subject to wind action has been investigated in sufficient detail, the strata have been found to be continually moving, either under the influence of wind or of internal seiches during the ensuing calm spells. Thermocline slopes of 1 m/km,

and more, have been frequently recorded; they were produced by moderate winds rarely exceeding force 6. In most cases the damping of the resulting seiche was small enough to allow oscillations of this order of amplitude to continue for days after the original disturbance. After what has already been said it will be unnecessary to emphasize the important influence of such displacements on the distribution of organisms and their food materials and on turbulent transport in general. Nor will the reader escape the conclusion that the interpretation of results from a single station, especially if it is situated some distance from the node, must take these movements into account. A warning to this effect was issued as early as 1901 by Ule (p. 140) in his classic essay on the physical limnology of the Starnbergersee, and was even more forcibly expressed by Wedderburn (1911, p. 628): 'They [the observations] should demonstrate to other observers the necessity for more careful investigation of lake temperatures and the futility of basing comparisons between lakes on observations made at one point and at considerable intervals of time.'

These warnings have, nevertheless, been largely unheeded; hydrobiologists have continued to draw doubtful conclusions from observations at single stations and at infrequent intervals. This failure to recognize the universal application of Wedderburn's work derives in part from the fact that no one since his day has organized temperature surveys in sufficient detail to distinguish between effects of wind and effects due to internal waves. The dispute which developed between Exner (1910) and Halbfass (1909, 1910*a*) over the interpretation of the latter's observations in the Mondsee may serve as an example. Halbfass believed that changes in the level of the isotherms were due to changes in the wind, and that internal seiches would not occur in unsettled weather. Exner held that Halbfass had not proved their absence in this case. Using Watson's equation, and inserting dimensions as defined in this paper, the period works out at about 25 h, somewhat longer than that calculated by Exner (1910), and the observations on 9 and 10 July 1909 (Halbfass 1909) are not inconsistent with an internal seiche of this period. But the following daily observations were so widely spaced that further progress of the seiche, if any, was unrecognizable. Birge (1910) also interpreted Wedderburn's early findings as the result of shifts in wind direction, and it is possible that his verdict of 'not proven' on Wedderburn's early work may have had some influence on subsequent opinion.

One is left with the impression that hydrobiologists, to whom advances in the science of limnology have largely been due, have usually regarded Wedderburn's 'temperature seiches' (in common with surface seiches) as an isolated phenomenon of interest to physicists, but not to themselves. This view they must now revise, for not only are the amplitudes sufficient to affect the whole economy of a lake, but, as this paper attempts to show, internal waves are the *universal* reaction of any enclosed basin of stratified water to wind impulses. Wedderburn (cf. 1911, p. 619) predicted this universality and, in an effort to convince sceptics that temperature seiches were to be expected in any stratified lake subject to wind action, he suggested to Halbfass that a joint Scottish and German expedition should investigate any lake of the latter's choosing. The result (Wedderburn 1911) was a striking and detailed demonstration of an internal seiche in the Madüsee. Halbfass was convinced (1910*b*).

Having recognized that the relatively small internal density differences in a lake permit moderate winds to displace the water layers considerably from their equilibrium positions,

the limnologist's interest in the internal seiches which these displacements initiate will centre round the flow pattern produced. This cannot yet be described from actual measurements of flow, but an attempt is made in this paper to deduce mean values at different levels in Windermere on a selected occasion (figure 22).

In passing, it may be noted that the few attempts so far made to measure flow at various depths fall into two classes. In the first the drift of floating or submerged objects, nets, etc., has been observed (Wasmund 1927–8; Mercanton 1932), and it is probable that seiche flow is the explanation of the appreciable subsurface drifts, often reversed in direction at increased depths, encountered during calm periods by the above observers, by fishermen and others. The second class is represented almost exclusively by Wedderburn and his collaborators. They used Ekman current meters, but found them generally too insensitive for recording movement below the thermocline. However, it seems likely that some of the hypolimnion currents in Loch Ness (Wedderburn & Watson 1909)—‘indications of secondary currents in the same direction as the wind below the temperature discontinuity’—and in Loch Garry (Wedderburn 1910, his figure 6) were in reality seiche currents or shifts due to changing winds.

*Flow in a two-layered basin*

As a first step we may consider the flow in a simple two-layered model, illustrated in figure 1, with dimensions and densities adjusted to the mean conditions obtaining in the northern basin of Windermere, during that interval (see figure 10) for which the most detailed temperature observations are available. The longitudinal sections (figures 9 and 11), as well as the preliminary comparison of observed and computed periods, show that the thermocline seiche is predominantly uninodal. The isotherm slopes are roughly uniform. We may therefore take our model lake to be a basin of rectangular cross-section, but variable depth (as figure 1), containing two homogeneous layers of mean thicknesses  $h_e$  and  $h_n$  and densities  $\rho_e$  and  $\rho_n$ , respectively, with a sharp interface between them. The period of the uninodal internal seiche is given by Watson's formula. It is easy to see that the volume transfer in each layer during the half-cycle  $c$  to  $g$  in figure 1 is, to a first approximation,  $\frac{1}{4}sl^2$ , where  $s$  is the maximum slope (assumed to be uniform) on the interface and  $l$  is the length of the basin measured along the interface. In a rectangular basin the mean depth of upper layer at the node is of course  $h_e$ , but in most lakes the mean depth of the hypolimnion at that section will be greater than the mean for the whole lake. The nodal mean we may call  $h_n$ . Then the mean nodal velocities in the upper and lower layers during the half-cycle we are considering are given by

$$sl^2/2Th_e \quad (3)$$

and

$$-sl^2/2Th_n, \quad (4)$$

respectively, where  $T$  is the period of oscillation. The difference in sign indicates that flow is opposite in direction in the two layers.

If we take a reasonable value of  $s$  from figure 10, and insert other mean values borrowed from later calculations, we have:  $h_e = 7$  m,  $h_n = 28$  m,  $l = 6.6$  km,  $s = 3.7 \times 10^{-4}$  (i.e. 1 m in 2.7 km—the distance from station  $P$  to the node),  $T = 19$  h =  $6.84 \times 10^4$  s. Formulae (3) and (4) then give the mean epi- and hypolimnion velocities, during the half-cycle we are considering, as 1.47 and  $-0.42$  cm/s respectively. These mean velocities are equivalent to

respective mean displacements of water at the node of 503 and 145 m per half-cycle. During the following half-cycle these displacements are of course reversed, but in a turbulent medium a water particle will, of course, rarely return to its original position. If we assume further that the motion is a simple harmonic one, then the maximum velocities at the node are  $\frac{1}{2}\pi$  times the above values, namely 2.31 and  $-0.66$  cm/s for the epi- and hypolimnion respectively. This gives a maximum velocity difference across the thermocline of *ca.* 3 cm/s. The above velocities and displacements are of course mean values and refer only to conditions at or near the node. As the ends of the lake are approached, horizontal amplitudes decrease and vertical displacements become more prominent.

*Internal waves in a three-layered basin*

The above rough estimates of velocity may not be far removed from reality as far as the epilimnion is concerned (see later discussion), but even a casual inspection of figure 10 will show that the hypolimnion estimates are quite misleading. The hypolimnion is clearly not, as assumed, a homogeneous layer. In fact this description can only reasonably be applied to the portion below the 20 m isobath. Between this and the thermocline—defined as the region of maximum density gradient—there lies a band of intermediate water, which we may call the metalimnion. The lower isotherms in this layer undergo large deflexions of complex wave-form, which can only be the result of considerable water movement.

The interpretation of these deflexions requires a theory of internal waves in a basin with more than two layers or, better still, a more general theory applicable to a basin in which density varies continuously with depth. Such a theory has been applied to progressive internal waves in the ocean by Fjeldstad (1933), but, as far as I know, it has yet to find application to standing waves in enclosed basins. As an *interim* step it is instructive to carry the analyses of the Windermere observations beyond the simple two-layer hypothesis and insert a third layer to represent an intermediate metalimnion. Makkaveev (1936) presents equations applicable to standing waves, neglecting friction, in rectangular basins containing three or more homogeneous layers of differing density. It is therefore possible, in theory, to improve the approximation to a natural lake by taking models with as many layers as necessary, but the complexity of the equations mounts rapidly as each additional layer is introduced.

A summary of the theory of oscillations in a basin with three layers is given as an appendix to this paper by M. S. Longuet-Higgins, to whom I am considerably indebted for advice and guidance in the computations which follow. Considering for the moment uninodal waves only, the equations show that there are three modes of oscillation. One is associated with the free surface and is in fact the well-known surface seiche; the other two are internal seiches associated with the two internal interfaces. Displacement at any one level is due to a combination of all three modes, but maximum displacement due to any one mode is found at the appropriate interface. In a model which approximates to lake conditions, the periods of the internal seiches will be very much longer than that of the surface seiche. In fact, the smaller the density difference across the interface, the longer will be the period of the mode associated with it. Displacement resulting from the surface mode (no. 1) is usually small enough to be neglected, and the periods of the internal modes (nos. 2 and 3) may be derived from equations (A 15) and (A 16) in the appendix and are given by

$$T^{(i)} = 2l / \sqrt{(-gH^{(i)})}, \quad (5)$$

where  $i$  denotes modality (2 or 3),  $l$  is the length of the basin,  $g$  is the acceleration of gravity, and  $H^{(i)}$  is one of the roots of the quadratic equation (A12) in the appendix. If the densities,  $\rho_1$ ,  $\rho_2$  and  $\rho_3$ , of the top, middle and bottom layers (of thickness  $h_1$ ,  $h_2$  and  $h_3$  respectively) are very near unity—as in lakes—this equation may be put into a more convenient form:

$$H^2(h_1+h_2+h_3) + H[h_1h_2(\rho_2-\rho_1) + h_2h_3(\rho_3-\rho_2) + h_1h_3(\rho_3-\rho_1)] + h_1h_2h_3(\rho_2-\rho_1)(\rho_3-\rho_2) = 0.* \quad (6)$$

This was used to obtain the results presented in Table 2. (It may be noted that if we set  $h_2=0$ , one of the roots of (6) is zero and the other is  $-h_1h_3(\rho_3-\rho_1)/(h_1+h_3)$ . With this inserted in (5) we obtain an equivalent of equation (2) for the two-layered case.)

The displacements experienced by both interfaces, and the free surface, are the result of superposition of all three modes in the proportions governed by equation (A13). In lakes, the displacement of the free surface is small enough to neglect in comparison with the displacements of the internal interfaces, and then the ratio of displacement of the upper interface to that of the lower is given for the second and third modes by equation (A14). The degree to which either mode is excited, i.e. the initial displacement from which oscillation starts, clearly depends on the history of the wind disturbance, and the picture is further complicated by the fact that any number of harmonics of both modes may be excited as well. The model experiment, illustrated in figure 20, provides an example of this. It will be discussed in more detail later. Again neglecting surface displacement, general expressions for deflexion of the interfaces (taking both modes and their possible harmonics into account) is given by the series (A17). When applying this to actual examples, coefficients for each harmonic term may be obtained from a Fourier analysis of the initial displacement of each interface under wind stress. This process is carried out in a following numerical example, in which the calculated displacements of selected isotherms are compared with observations. Before proceeding to this it is helpful to examine briefly the effect of wind stress on a three-layered basin.

#### *The response of a three-layered basin to wind stress*

This problem has been considered by Hellström (1941). He showed that, if the wind has been blowing long enough to set up the steady state indicated in figure 13*a*, then it is possible to calculate the slopes on the water surface and on the interfaces, and also to compute the velocity distribution, if the drag on the water surface can be assessed and the coefficient of turbulent diffusion in each layer is known. The equations are somewhat complex, but if turbulence in the middle layer approaches zero they become much simpler. This is a reasonable approximation to nature because of the high stability in this layer. The result is a small uphill slope on the water surface to the leeward, too small to show in figure 13, and a much larger—by a factor  $\rho_1/(\rho_2-\rho_1)$ —downhill slope,  $S_2$ , on the upper internal interface. To arrive at this state, the middle layer must be displaced windward, but as long as the bottom layer still remains protected from direct contact with the circulation in the top layer, the lower interface remains horizontal as indicated in figure 13*a*. This conclusion was borne out by model experiments in which wind stress was applied to

\* Equation (6), and also equation (8) on p. 385, is dimensionally correct only if the densities are expressed in c.g.s. units.

a tank containing three layers: water, phenol and a 25% glycerine solution. This model basin, which had the form and dimensions illustrated in figure 14 (further details in Mortimer 1951), was contained between plate-glass sides 10 cm apart. Three blowers at *B* were spaced to give a roughly uniform wind distribution along the water surface. The experiment was designed to give only qualitative indications of the response of a three-layered basin to wind stress, and no precise measurements of wind speed were made. It was found, however, that steady winds of the order of 1 m/s or less near the water surface

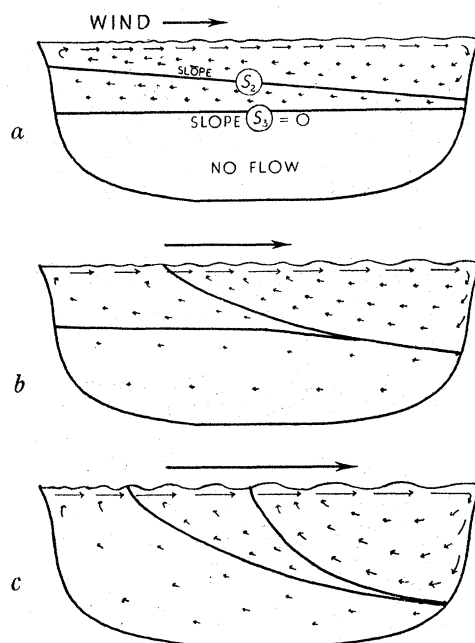


FIGURE 13. Movement caused by wind stress in a hypothetical three-layered lake, (a) with a steady moderate wind, (b) and (c) with more violent winds. Direction and velocity of flow are indicated roughly by arrows.

produced, after a minute or so, the steady states (illustrated in figure 14*a* and *b*) predicted by Hellström (1941), in which the lower interface and the bottom layer were not disturbed, while the upper interface was tilted to a degree dependent on wind strength. Strong circulation was maintained in the upper layer, while the two lower layers were nearly stationary. This condition is reminiscent of that in lakes (cf. figures 8 and 21) in which steady winds produce a very sharp thermocline at the leeward end, in contrast to a spreading out of the isotherms at the windward end of the basin.

Conditions produced by stronger winds, and illustrated in figure 14*c* and *d*, are discussed later.

Reliable estimation of wind drag on water surfaces is still a matter of some difficulty, and the answer seems to vary considerably with the method used (Charnock 1951). Recent estimates for sea conditions were made by Munk & Anderson (1948), and Hellström's estimate of drag (proportional to  $w^{1.8}$ , where  $w$  is the wind speed at 6 m above the water surface) fit these reasonably well. Combining Hellström's equations (141) and (160) and taking account of his remarks on p. 113, we find that the fully developed slope of the upper interface, looking to windward, is given by

$$s_2 = (3.7 \times 10^{-2} cw^{1.8}) / g(\rho_2 - \rho_1)h_1, \quad (7)$$



in which  $w$  is defined as above and measured in m/s, the terms in the denominator are in c.g.s. units, and  $c$  ranges between 1 and 1.5, depending on assumptions made about flow and turbulence in the top layer. Without pursuing the matter more closely, we may expect the interface slope to vary in rough proportion to the square of the wind speed, and in

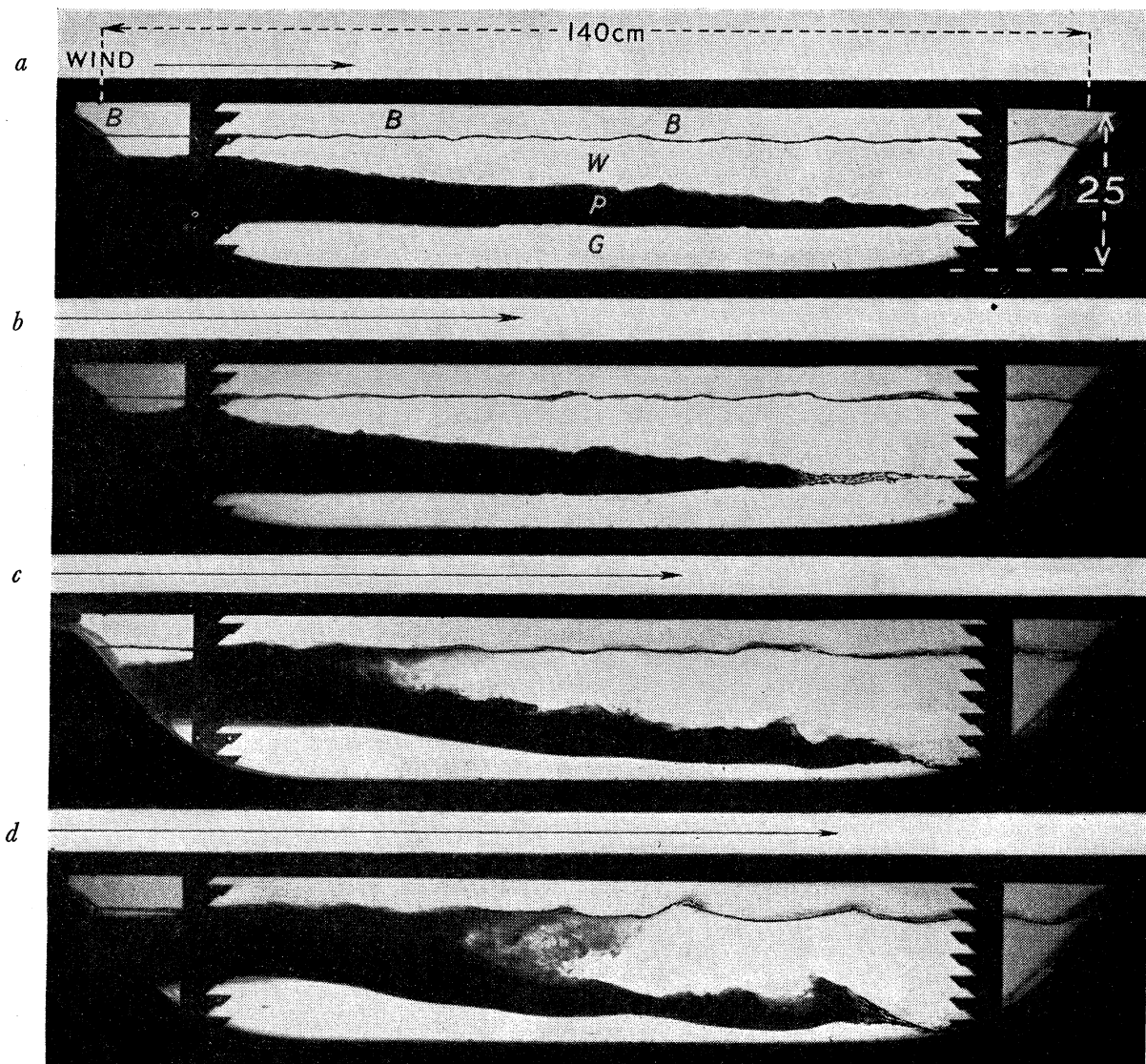


FIGURE 14. The effect of wind stress on a model lake containing three layers of differing density. Wind force is indicated roughly by the length of the arrows; (a) and (b) steady moderate winds, (c) and (d) more violent winds. Blowers were situated at  $B$ . The fluids used, and their approximate densities, were: water ( $W$ ) 1.00, commercial cresol ( $P$ ) 1.04 and 25% glycerine solution ( $G$ ) 1.06.

inverse proportion to the thickness of the top layer and to the density difference between top and middle layer. In view of the doubt which still attaches to estimates of the relation between drag and wind speed, (7) should only be regarded as an approximate guide.

In passing it may be pointed out that the thermocline slopes observed in figures 5, 7 and 8 are all, with the possible exception of figure 7, considerably less than those estimated from (7). This does not necessarily point to inadequacies in the theory, but may be due to

a variety of causes: over-estimation of mean wind velocity, the fact that the fetch was not long enough to allow the full drag to develop, or that the time of blow was not long enough to build up the maximum slope. It is clear that time relations are important here, and it is hoped that more detailed observations with adequate wind data will be made in future. In this connexion, the results of a theoretical investigation by Proudman & Doodson (1924) of the time relations of meteorological effects on the sea surface may be applied. They showed that under certain conditions the surface slope set up by wind stress may first oscillate about its final steady-state value.

There is an obvious limit to the magnitude of  $s_2$ , or its equivalent in lakes, and Hellström's investigations do not cover what happens when this limit is exceeded. But it may be assumed that the steady states illustrated in figures 13*a* and 14*a* and *b* will only persist as long as the slope of the upper interface does not become so steep that either it cuts the free surface at the windward end, or allows top and bottom layers to come into direct contact at the leeward end. If the first event occurs, middle water will become caught up in the surface wind-drift and mixed into the upper layer. In the second event, the bottom layer, now in direct contact with the circulating top layer, is also dragged to windward. This will lead to the condition indicated in figure 13*b* and *c* and that produced by strong winds in the model experiment, figure 14*c* and *d*. This condition in the model, and its counterpart in the lake under gale stress (figure 8), cannot be regarded as steady states except in a limited sense, for water from subsurface layers is continually mixing into the top layer as long as the strong wind continues. The top layer will thus gain in volume and increase in density (compare, for example, figures 21 and 8). The model also showed that distribution of the layers greatly depended on how the wind stress was built up. As we have seen, steady, moderate winds produced the 'steady states' shown in figure 14*a* or *b*. A slow build-up to a strong wind could produce a distribution similar to 14*b*, but a sudden onset of wind of the same strength displaced both interfaces and led to the condition illustrated in 14*c* or *d*. This is clearly a complex state of affairs, but one likely to repay further study, if the dynamics of stratified lakes are to be understood.

*A comparison of the internal wave pattern observed in Windermere with that computed for a three-layered basin*

As it appears that figure 8 is fairly consistent with a picture of a three-layered basin under wind stress, it may be of value to compare the observed internal waves (figure 10), which followed the gale, with those computed for a hypothetical three-layered basin in which the density distribution and dimensions have been fitted to mean lake conditions. The assumptions involved in making such a fit are discussed in detail later, and in order to apply the theory given in the appendix it must further be assumed that the starting conditions for the oscillations are known. In this case figure 8*b* has been taken as an approximate steady state from which the waves proceeded.

To arrive at the nearest fit to density distribution in the lake we may take (i) an approximate mean vertical temperature distribution derived from the longitudinal sections (figures 9, 11) on 10 and 13 June and (ii) a similar distribution at station *P* derived from figure 10 for the interval 10 to 13 June. Figure 15, right-hand side, shows that differences between estimates (i) and (ii) are small. Then, making the assumption, valid for most lakes,

that density depends entirely on temperature, an equivalent mean curve of vertical density distribution is derived on the left-hand side of figure 15. The manner in which a two-layered or a three-layered model may be fitted to this curve is also indicated. The upper layer of thickness  $h_1$  (or  $h_e$  in the two-layered case) is common to both models. The thicknesses of the bottom layers ( $h_3$  in the three-layered and  $h_h$  in the two-layered model)

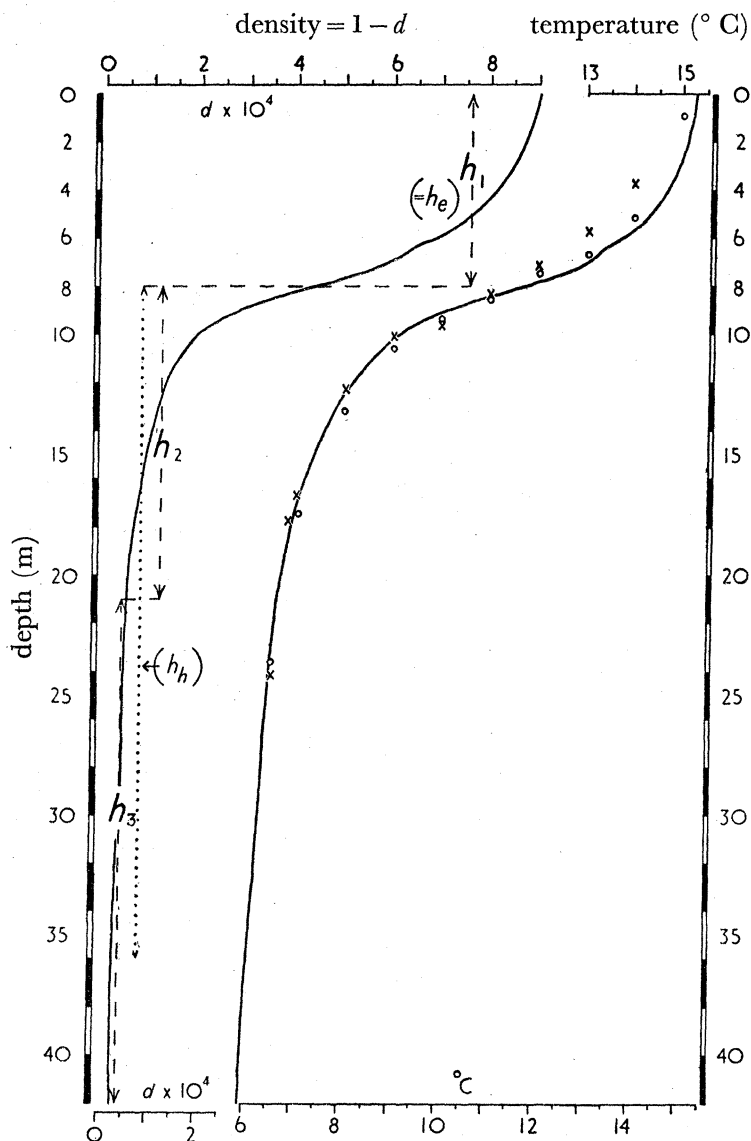


FIGURE 15. Mean vertical distribution of temperature and density at station *P*, Windermere northern basin, during the interval 10 to 13 June 1947, and also the mean vertical distribution of temperature in the whole basin on 10 June a.m. (x) and 13 June p.m. (o). The figure also shows the way in which hypothetical two-layered ( $h_e$  and  $h_h$ ) and three-layered ( $h_1$ ,  $h_2$  and  $h_3$ ) models were fitted to the density distribution.

are taken as the mean depth of the lake basin, derived from figure 16, below the appropriate interface ( $h_e/h_h$  or  $h_2/h_3$ ). It is convenient in what follows to refer to each layer by its equilibrium thickness,  $h_1$ ,  $h_2$  and  $h_3$ , and to the interfaces as  $h_1/h_2$  and  $h_2/h_3$  respectively.

In choosing the equilibrium levels of the two interfaces we are faced with the difficulty that, whereas the layers in the model are assumed to be of uniform density, those in the

lake are not. In many lakes  $h_1$  and  $h_3$  may be taken to coincide fairly well with a homogeneous, well-mixed epilimnion and a nearly uniform deep-water layer, the bathylimnion.

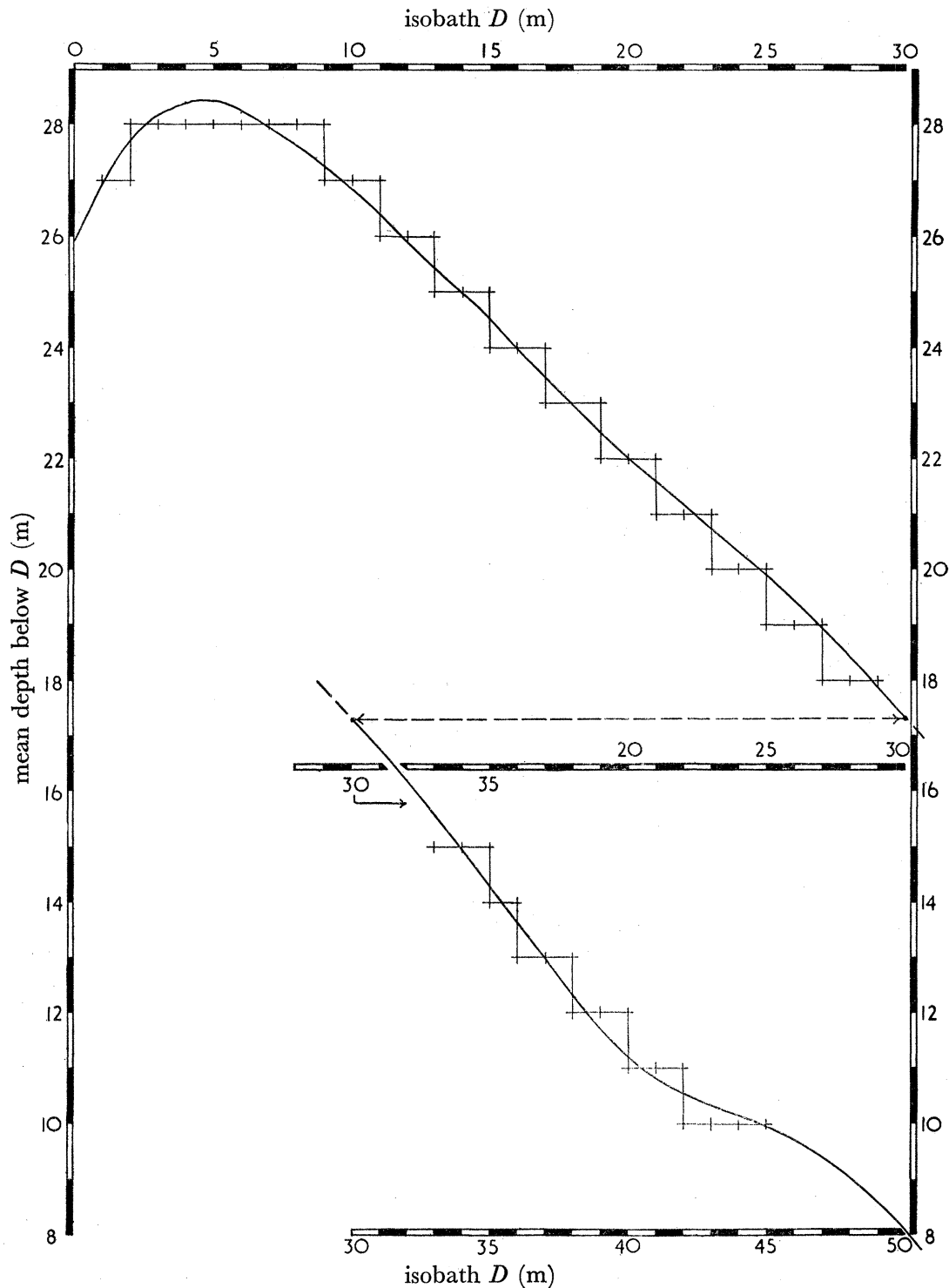


FIGURE 16. Windermere northern basin: mean depth below any isobath ( $D$ ) within the range 0 to 50 m, derived from the 1937 Admiralty echo-sounding survey.

The  $h_1/h_2$  interface will therefore be easily located at the level of maximum density gradient in the thermocline. (The fit, in figure 15, to mean conditions at station  $P$  for the whole

interval 10 to 13 June is more difficult than it would be for a shorter interval, because of changes in level of the thermocline and the effect of surface heating and mixing.) But difficulties arise in choice of level for the  $h_2/h_3$  interface, because in nature there is rarely any discontinuity between the middle and bottom water. However, as we shall see later, variation in choice of level of the lower interface does not affect the period calculation to any large extent.

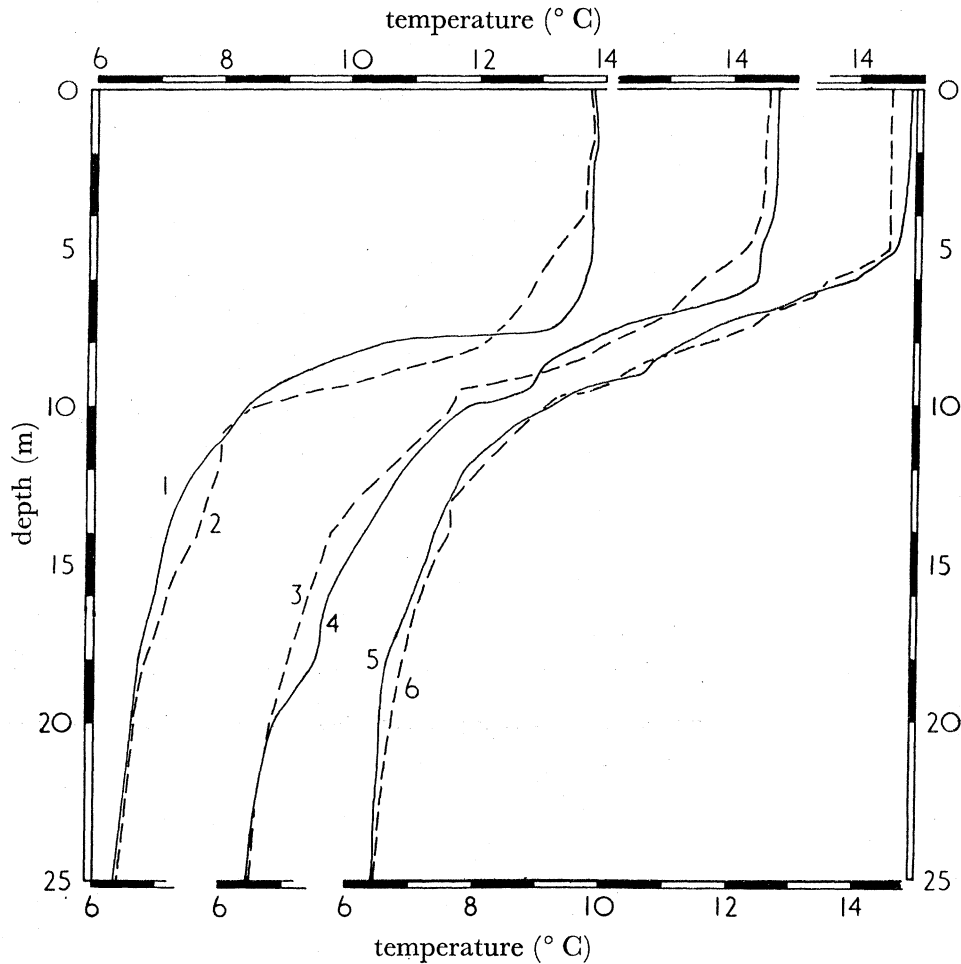


FIGURE 17. Vertical temperature profiles at stations *P* and *B*, Windermere northern basin, compared: nos. 1 and 2, 11 June 1947, *P* 08.00 and *B* 07.30 h, respectively; nos. 3 and 4, 12 June, *P* 14.00 and *B* 14.36 h, respectively; nos. 5 and 6, 13 June, *P* 11.17 and *B* 10.46 h, respectively.

A closer examination of figure 10 will show that, as far as the thermal structure of the epilimnion and thermocline is concerned, the period under review may be divided into three roughly equal sections. During the first 24 h there was little surface heating, and the thermocline was very sharp. During the two hot days which represent the middle section the surface layers gained considerable heat. In the last section, 13 June, this heating combined with cooling and convection at night, and with mixing across the thermocline, had produced a vertical density distribution considerably different from that in the first section. It may be mentioned in passing that mean conditions for the last section are very close to mean conditions for the whole lake computed from the longitudinal section on 13 June (figure 11). But the same cannot be said of the comparison between the mean for

the first section and the mean for the whole lake calculated from the longitudinal section on 10 June (figure 9). The thermocline was sharper at station *P* than at other stations. In the absence of longitudinal sections during the period covered by figure 10, when hourly observations at station *P* were in progress, it is impossible to say how far mean conditions at station *P* differed from mean conditions for the whole basin. But it was

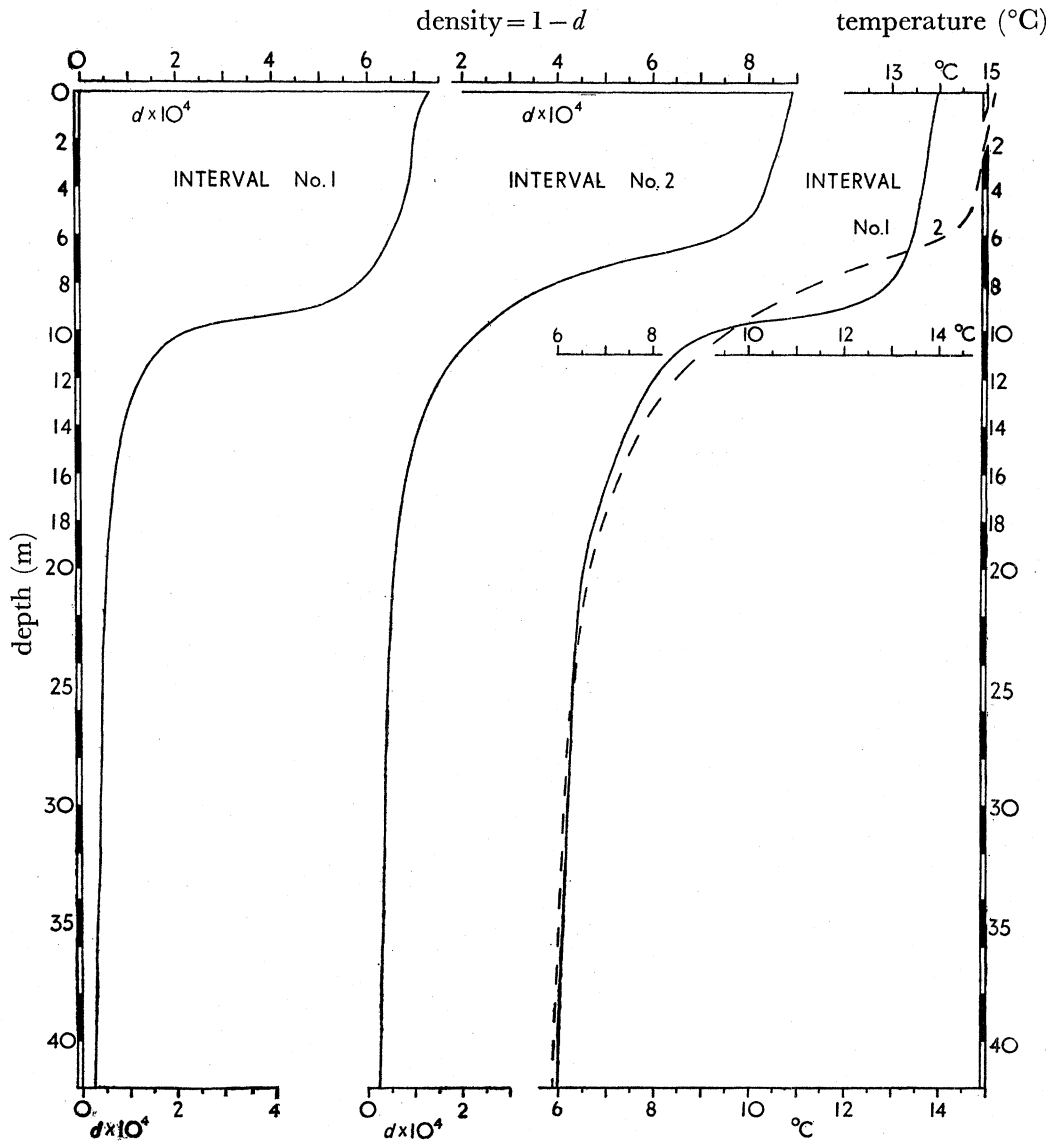


FIGURE 18. Mean vertical distribution of temperature and density at station *P*, Windermere northern basin, during the 19 h intervals (nos. 1 and 2) indicated in figure 10.

possible to obtain occasional profiles at station *B*; figure 17 compares these with profiles at *P* within the same half-hour. The *B* and *P* profiles were fairly similar on 12 and 13 June, but again there was a much sharper thermocline at *P* on 11 June.

Neglecting the middle section of figure 10, in which the epilimnion is not homogeneous, an attempt has been made to fit three-layered models to the mean vertical density distributions during the first and last sections, cf. figure 18. To eliminate the effect of the thermocline oscillation as far as possible, mean levels were computed for each isotherm over

a 19 h interval, so chosen that the lower isotherms were not greatly deflected from their mean position. This should give the best possible mean in the circumstances. The two intervals, chosen as representative of the first and last sections, are indicated as no. 1 and no. 2 respectively in figure 10. The mean distributions of temperature for these intervals are illustrated, superimposed to illustrate mixing, at the right-hand side of figure 18. It was again considered sufficiently accurate to compute the mean density distributions (figure 18, left-hand side) from these temperature curves.

TABLE 2. CALCULATED PERIODS OF INTERNAL MODES IN THREE-LAYERED MODELS FITTED TO MEAN CONDITIONS IN WINDERMERE NORTHERN BASIN DURING THE INTERVAL FROM 11.00 h ON 10 JUNE TO 15.00 h ON 13 JUNE 1947, AND FOR TWO SHORTER, SELECTED 19 h INTERVALS (SEE FIGURE 10). THE PERIOD IS ALSO CALCULATED FOR EQUIVALENT TWO-LAYERED MODELS (A SINGLE MODE IN THIS CASE). THE TABLE ILLUSTRATES THE EFFECT OF VARYING CHOICE OF THE EQUILIBRIUM LEVEL OF THE INTERFACES. THE LAST LINE IN THE TABLE REFERS TO THE MODEL FITTED TO THE DENSITY DISTRIBUTION IN FIGURE 15.

interval	data used in the calculations						period of mode (h)		
	three-layered model			two-layered model*			three-layered case		two-layered case
	interface depth (m) †		density diffs × 10 <sup>4</sup>			thickness of $h_h$ (m)	third mode	second mode	single mode
	$h_2/h_3$	$h_1/h_2$	$(\rho_3 - \rho_2)$	$(\rho_2 - \rho_1)$	$(\rho_h - \rho_e)$				
no. 1, 19 h	21	8.5	0.90	5.40	5.90	27.5	46	18.6	19.0
centred on	21	9.0	0.75	5.45	5.85	27	51	18.3	18.6
21.30 h, 10 June	21	9.5	0.60	5.50	5.80	26.5	57	18.0	18.4
no. 2, 19 h	21	6.0	1.55	6.55	7.25	29	34	19.0	19.3
centred on	21	6.5	1.40	6.55	7.20	28.5	36	18.6	18.9
21.00 h,	21	7.0	1.25	6.55	7.15	28	38	18.2	18.6
12 June									
whole interval	21	7.0	1.05	6.55	7.05	28	41	18.3	18.8
10 to 13 June	20	7.0	1.15	6.45	7.05	28	40	18.3	18.8
	21	8.0	0.80	6.40	6.80	28	47	17.7	18.0

\*  $h_e/h_h$  interface at same depth as  $h_1/h_2$ .

† The length  $l$  is taken as 6.6 km for all interfaces, and the thickness of layer  $h_3$  is taken as the mean depth (cf. figure 16) below the  $h_2/h_3$  interface, i.e. 22 m in the last but one entry and 21 m in all others.

Taking  $l$  as 6.6 km for both interfaces, and using values of  $h_1$ ,  $h_2$ ,  $h_3$ ,  $\rho_1$ ,  $\rho_2$  and  $\rho_3$  derived from figures 15 and 18, we may proceed to the period calculations using equations (5) and (6). As in figure 15, it is also clear in figure 18 that the choice in level of the  $h_1/h_2$  and  $h_2/h_3$  interfaces could vary within narrow limits. To illustrate the effect of such variation, the calculated periods for the two modes (and for the single mode in the two-layered case) are presented in table 2 for a range of values of  $h_1$ , etc. In what follows, it will be convenient to refer to the modes associated with  $h_1/h_2$  and the  $h_2/h_3$  interfaces as the *second mode* and *third mode* respectively.

Table 2 shows that the calculated period of the second mode is little affected by variation of choice of level for the  $h_1/h_2$  interface, apparently because any shortening of the period due to increasing the thickness of  $h_1$  is largely balanced by the decrease in the value which must be assigned to  $(\rho_2 - \rho_1)$ . The calculated period is in close agreement with the

observed period of about 19 h and also differs little from that calculated for a two-layered model by Watson's formula. In other words the period of the second mode is largely independent of the density structure at sub-thermocline levels and depends mainly on differences in mean density above and below the thermocline. This explains the success with which Watson's simple formula has predicted the period of thermocline oscillations in other cases, but of course it can give no information on events below the thermocline.

The calculated period of the third mode, on the other hand, shows greater change with varying choice of the  $h_1/h_2$  level, largely because of the influence this choice has on the value assigned to  $(\rho_3 - \rho_2)$ . Change in level of the  $h_2/h_3$  interface (bottom section of table 2) affects the period less. Perhaps the most important result of the above calculations is that, in spite of the errors inherent in the assumption of an homogeneous middle layer, the predicted period of the third mode is consistent with the observed deflexion of 40 to 50 h period in the lower isotherms. During the two shorter intervals (1 and 2), the calculated period of the third mode is respectively longer and shorter than that for the whole interval. The result clearly depends greatly on the value assigned to  $(\rho_3 - \rho_2)$ . The observations in figure 10 were not extended long enough to decide whether a progressive decrease in period of the third mode did in fact occur.

We may now examine the partition of the modes between the two interfaces. Using equation (A14), it is possible to calculate the ratio,  $\beta$ , of vertical displacement of the upper to that of the lower interface for each mode. As the densities are very nearly unity, (A14) may be recast into a more convenient form:

$$\beta^{(i)} = (h_2/H^{(i)})(\rho_3 - \rho_2) + (h_2/h_3 + 1), \quad (8)$$

in which  $i$  = modality, 2 or 3, and  $H^{(i)}$  is a root of (6). Using the entries in table 2, the ratio  $\beta^{(2)}$  for the second mode varies between 1.30 and 1.39 for interval no. 1, between 1.10 and 1.23 for interval no. 2 and between 1.23 and 1.38 for the whole interval. The respective ranges of the ratio  $\beta^{(3)}$  for the third mode are: -0.13 to -0.08, -0.22 to -0.15 and -0.10 to -0.14. There is no need to set all these values out in detail, but if we give greatest weight to the last entry in table 2 (equivalent to figure 15), we may accept the values  $\beta^{(2)} = 1.30$  and  $\beta^{(3)} = -0.12$  for subsequent calculations. (Identical values are arrived at, if mean conditions for the longitudinal section, figure 8*b*, on the afternoon of 9 June are utilized.) We may therefore expect (i) that, for unit deflexion due to the 19 h mode at the upper interface, there will be a corresponding in-phase deflexion with amplitude 0.77 at lower levels, and (ii) that, superimposed on the 19 h oscillation at the thermocline, there will be a wave of much longer (40 to 50 h) period, opposite in phase and with about one-eighth of the amplitude of the long-period wave in the lower isotherms. Briefly, both predictions are roughly borne out by the observations (figures 10, 19). Effect (ii), for instance, provides a hitherto unsuspected explanation of the apparent shift in the mean level of the thermocline oscillation, clearly seen during the first half of figure 10. The magnitude and sign of this shift is indicated by a dotted line in figure 19*b*.

Having calculated the values  $T$  and  $\beta$ , and taking figure 8*b* to represent the initial disturbance, we may now compute subsequent interface displacements at any point in the lake; here we select station  $P$ .

Figure 8*b* illustrates the isotherm distribution shortly before the wind dropped, at which time the wind had been blowing for about 12 h. This is taken as the best available picture



of the steady state, under wind stress, from which the oscillations originated. The first step is to carry out a Fourier analysis of the initial displacement of each interface from its equilibrium level. The  $11^\circ$  and  $6.7^\circ$  isotherms may be considered to occupy sufficiently closely for our purpose the respective positions of the upper and lower interface (see figures 15, 18). These isotherms are drawn as heavier lines in figure 10. From their mean levels we have:  $h_1 = 8.5$  m,  $h_2 = 12$  m and  $h_3 = 21.5$  m (from figure 16). The result of the Fourier analysis of the deflexions of the  $11^\circ$  and  $6.7^\circ$  isotherms from these mean levels during the afternoon of 9 June is indicated in figure 8*b*. For our purpose it is sufficiently precise to carry the analysis as far as the third harmonic only. There is close agreement between this result and the actual course of the isotherms. The Fourier coefficients obtained in this way supply, with the help of equations (A22) and (A23), the respective coefficients for insertion in the displacement equations (A17). These are inserted in round brackets in (9) and (10) below because they will be needed later. With appropriate values of  $\sigma^{(i)} = 2\pi/T^{(i)}$  for each mode, the equations (A17) give the displacement (downwards being positive) of both interfaces from their equilibrium level in any transverse plane at distance  $x$  along the longitudinal section, and at any time,  $t$ . The periods  $T^{(2)}$  and  $T^{(3)}$  have already been given by (5) and (6). At station  $P$  we have

$$k_0x = \pi x/l = 0.286, \quad \cos k_0x/l = 0.96, \quad \cos 2k_0x/l = 0.84, \quad \cos 3k_0x/l = 0.66.$$

We have also assumed that figure 8*b* represents a state of rest from which the oscillations started. Then the sine terms vanish in (A17), and, taking  $\beta^{(2)} = 1.3$  and  $\beta^{(3)} = -0.12$ , the deflexion in metres of the  $11^\circ$  and  $6.7^\circ$  isotherms at station  $P$  are given by

$$\begin{aligned} \zeta_{11^\circ, P} = & 1.3[(2.00) 0.96 \cos \sigma^{(2)}t + (0.42) 0.84 \cos 2\sigma^{(2)}t + (0.44) 0.66 \cos 3\sigma^{(2)}t] \\ & - 0.12[(4.39) 0.96 \cos \sigma^{(3)}t + (2.19) 0.84 \cos 2\sigma^{(3)}t + (0.89) 0.66 \cos 3\sigma^{(3)}t] \end{aligned} \quad (9)$$

and

$$\begin{aligned} \zeta_{6.7^\circ, P} = & [(2.00) 0.96 \cos \sigma^{(2)}t + (0.42) 0.84 \cos 2\sigma^{(2)}t + (0.44) 0.66 \cos 2\sigma^{(2)}t] \\ & + [(4.39) 0.96 \cos \sigma^{(3)}t + (2.19) 0.84 \cos 2\sigma^{(3)}t + (0.89) 0.66 \cos 3\sigma^{(3)}t] \end{aligned} \quad (10)$$

To derive  $\sigma^{(i)}$ , the periods  $T^{(2)} = 19$  h and  $T^{(3)} = 41$  h are chosen as a reasonable fit, both with observations (figure 10) and calculations (table 2). The calculated levels of the  $11^\circ$  and  $6.7^\circ$  isotherms are then compared with those observed in figure 10. This comparison is made in figure 19 for an interval of 96 h from  $t = 0$  at 17.00 h on 9 June until the end of the interval covered by figure 10. It will now be more convenient to refer, in what follows, to the second and third mode as the 19 and 41 h wave respectively. The comparison for the  $11^\circ$  isotherm requires little comment; for, even with considerable latitude of choice of variables in table 2, the calculated period is always close to 19 h and the oscillation is largely unimodal, a prediction which is also made by the two-layer theory, and one which clearly fits the observations closely. The novel result of this application of three-layer theory is the correspondence, in main features at least, of the calculated and observed deflexions of the lower ( $6.7^\circ$ ) isotherm.

As the theory takes no account of friction, it is not surprising that the ratio of observed to calculated amplitude becomes less with increasing time in figure 19*a*. Although there is not sufficient knowledge to apply valid corrections for friction, it is nevertheless of interest to apply an arbitrary damping factor to both modes, and to each of their harmonics,

estimated to achieve the best agreement between calculated and observed amplitudes. Figure 19*b* illustrates such an attempt, in which a logarithmic decrement of 0.26 per cycle (equivalent to an amplitude reduction of 23 % per cycle) is applied to the fundamental and each harmonic of both modes. For the 11° isotherm the correspondence is good, and it appears that the theory, in part at least, can account for the variations in mean level

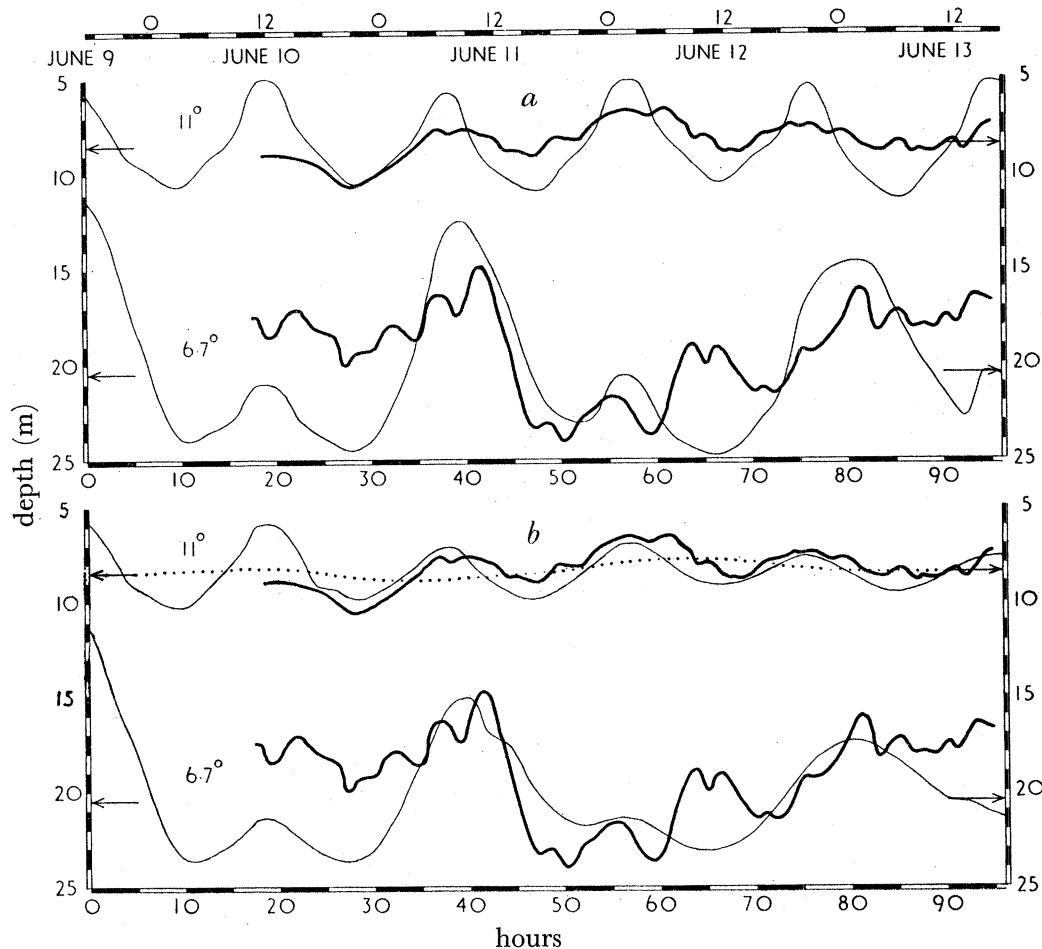


FIGURE 19. Variation in depth of the 11° and 6.7° isotherms at station *P*, Windermere northern basin, derived from observation (thick lines) and theory (thin lines), during an interval of 96 h starting at 17.00 h on 9 June 1947. The theoretical values are uncorrected for damping in 19*a*; in 19*b* an arbitrary damping coefficient (log. decrement 0.26 per cycle) is applied equally to each mode and to each of their harmonics. Mean levels are indicated by arrows. The dotted line in 19*b* roughly indicates a general shift in level of the 11° isotherm (cf. text).

of the thermocline already mentioned and roughly indicated by a dotted line in figure 19*b*. We have assumed that the damping factor applies equally, per cycle, to all harmonics. It follows that the higher the harmonic, the more rapid will be its damping in time; the fundamental will therefore persist the longest. A complex initial disturbance will, in the absence of further wind, eventually develop into a pure uninodal seiche. Although this assumption seems a reasonable one, it should be pointed out that in the one example examined on this point (Wedderburn & Young 1915) the uninodal internal seiche

appeared to be damped more rapidly than its binodal harmonic (their figure 17). There were, however, disturbances due to wind which, in their view, affected the binodal seiche disproportionately. Neither is the point settled by figure 19, because the observed course of the 11° isotherm is obscured by the superposition of waves of 2 to 3 h period and of unknown origin. The agreement between theory and observation in figure 19*b* may, however, suggest that the damping coefficient we have chosen is not far removed from that which was operative in Windermere. The uninodal internal seiche in Loch Earn (Wedderburn & Young 1915) appears to have been somewhat more highly damped than in our case. Figure 19*b* suggests that the 41 h wave may have been less damped than we have assumed, and the 19 h wave slightly more so. This result, if it is significant, may be attributed to the presence (to be demonstrated later) of the steepest velocity gradients in the thermocline region. The relative persistence of long-period waves in deeper water will be mentioned again.

The three-layered model described earlier can also be used to demonstrate internal waves which follow a wind disturbance. The top picture in figure 20 is one taken under wind stress with conditions essentially the same as in figure 14*c*. Successive stages in the internal waves which followed when the wind had been stopped clearly show that higher harmonics, prominent at first, were damped out more rapidly than the two fundamental waves on the two interfaces.

The theory applied above not only ignores friction; it equally ignores its concomitant—mixing. An obvious result of mixing is the spreading of the isotherms observed at thermocline level as time proceeds in figure 10. This may have contributed to the slight rise in ‘mean’ level of the 11° isotherm, and may also have led to an increase of friction at thermocline level. Otherwise the effects of mixing would appear to be of a second order compared with the deflexions of isotherms by internal waves; this is borne out by the similarity (figure 15) of the mean vertical distribution of temperature in the basin on 10 and 13 June.

One interesting conclusion from the foregoing analysis is that, with suitable starting conditions (e.g. figure 8), waves of large amplitude and long period can persist in the lower layers for a long time with a lower rate of damping (per unit time) than the internal seiche at thermocline level. For instance, figure 10 happens to finish with the 11° and 6.7° isotherms both deflected upward at station *P*. A longitudinal section (figure 11) investigated at this time shows that the thermocline and the lower isotherms were sloping in the same direction, a condition consistent with two uninodal modes more or less in phase. An out-of-phase picture is not available for this series, but a longitudinal section on 4 June (figure 21*a*) illustrates this condition in an oscillation which was probably started on 28 May (see figure 5). Apart from showing the way in which isotherms in upper and lower metalimnion may slope in opposite directions, figure 21 also illustrates the action of wind in mixing and deepening the epilimnion after several days of hot calm weather, apparently in this case without much modifying an existing oscillation in the lower isotherms. By the next day (5 June, figure 21*b*), as might be expected with an oscillation of 40 to 50 h period, the lower isotherms were sloping in the opposite direction. Incidentally, a comparison with the longitudinal section 4 days later (figure 8) also shows how strong winds, culminating in a gale, continued to cool and deepen the epilimnion.

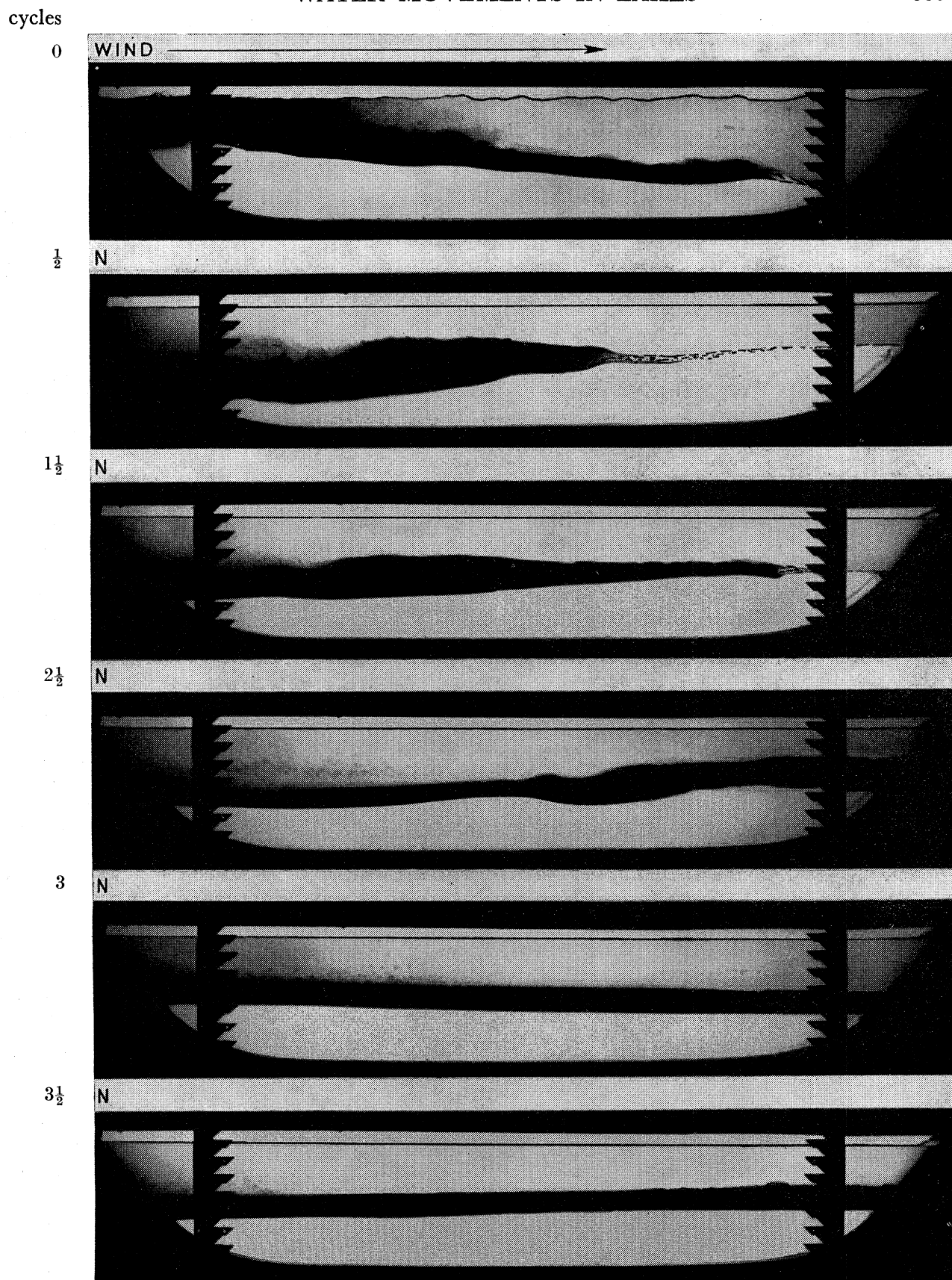


FIGURE 20. Internal waves, after wind stress, in a model lake with three layers of differing density (for details of the layers see figure 14). The initial condition under wind stress is shown in the top picture; the lower pictures ( $N$  = no wind) illustrate successive stages in the oscillations which followed after the wind had stopped. The number of cycles through which the main oscillation had passed are given on the left of the figures.

*Predicted flow in a three-layered model applied to Windermere*

A further application of the theory given in the appendix—and one which will probably be of more direct interest to hydrobiologists than the foregoing prediction of isotherm deflexions—is the calculation of flow in each layer. Neglecting the rotation of the earth and the detailed structure of turbulent flow, the mean flow produced by longitudinal internal seiches will always be parallel to the longitudinal axis of the basin. Near the nodes this flow is horizontal, but as the ends of the basin are approached, vertical components become more marked.

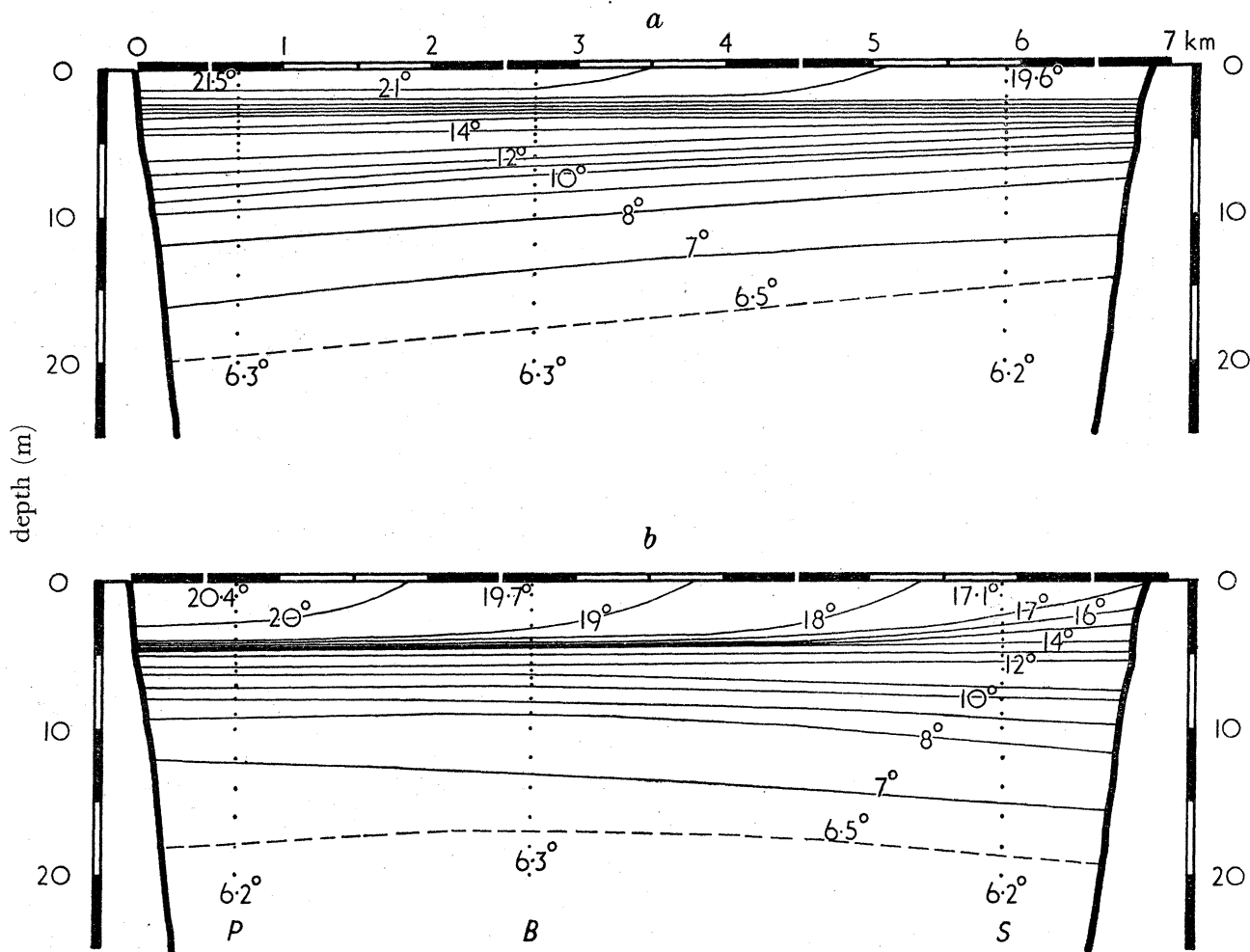


FIGURE 21. Distribution of temperature in a longitudinal section of Windermere northern basin on (a) 4 June 1947 (15.21 to 16.40 h) when a south-east wind was starting to blow after several hot calm days, and (b) 5 June 1947 (09.15 to 10.46 h) at which time the south-east wind had been blowing at force 5 to 6 overnight. Letters indicate measuring stations. The vertical scale is  $100 \times$  the horizontal.

General expressions for the horizontal components of flow at any point,  $x$ , in the basin and at any time,  $t$ , are given for each layer by (A24), (A25) and (A26). It will be observed that, apart from differences in sign, the coefficients,  $A_n^{(i)}$  ( $i$ =modality, 2 or 3;  $n$ =harmonic number) are the same as in the equations of interface displacement (A17). Therefore to calculate horizontal flow in the numerical example covered by (9) and (10),

we have only to transfer the equivalent values of  $\beta^{(i)}$ ,  $\sigma^{(i)}$  and the coefficients  $A_n^{(i)}$ . At the central transverse plane of the basin, i.e. the uninode where  $x = \frac{1}{2}l$ , the flow equations simplify to (A27) and (A28). In this plane, flow is zero for the even harmonics. The cosine terms also vanish if we assume a start from rest. For this case the flow equations become

$$u_1 h_1 = \beta^{(2)} \sigma^{(2)} l \pi^{-1} (2.00 \sin \sigma^{(2)} t - 0.44 \sin 3\sigma^{(2)} t) + \beta^{(3)} \sigma^{(3)} l \pi^{-1} (4.39 \sin \sigma^{(3)} t - 0.89 \sin 3\sigma^{(3)} t), \quad (11)$$

$$-u_3 h_3 = \sigma^{(2)} l \pi^{-1} (2.00 \sin \sigma^{(2)} t - 0.44 \sin 3\sigma^{(2)} t) + \sigma^{(3)} l \pi^{-1} (4.39 \sin \sigma^{(3)} t - 0.89 \sin 3\sigma^{(3)} t), \quad (12)$$

$$u_2 h_2 = -(u_1 h_1 + u_3 h_3), \quad (13)$$

and for this numerical example, taking the layer thicknesses as before ( $h_1 = 8.5$  m,  $h_2 = 12$  m,  $h_3 = 21.5$  m), the velocity in cm/s is given by

$$u_1 = (5.90 \sin \sigma^{(2)} t - 1.30 \sin 3\sigma^{(2)} t) - (0.55 \sin \sigma^{(3)} t - 0.11 \sin 3\sigma^{(3)} t), \quad (14)$$

$$-u_3 = (1.80 \sin \sigma^{(2)} t - 0.40 \sin 3\sigma^{(2)} t) + (1.84 \sin \sigma^{(3)} t - 0.37 \sin 3\sigma^{(3)} t), \quad (15)$$

$$u_2 = -(8.5u_1 + 21.5u_3)/12.0. \quad (16)$$

As in (9) and (10) it is only necessary to consider the first three harmonics. The negative signs before (12) and (15) result from a convention that flow is positive in a northerly direction in this example.

The results are presented in figure 22. There are two sets of curves; one neglects damping, the other introduces the damping coefficient applied in figure 19*b* (i.e. a logarithmic decrement of 0.26 cycle on both modes and all harmonics). The assumptions made, in addition to those introduced in the preparation of figure 19, are (i) that  $h_1$ ,  $h_2$  and  $h_3$  are invariable at the uninode, and (ii) that the thickness of the bottom layer at the uninode is the same as that for the whole basin, i.e. equal to  $h_3$ . This latter condition only holds approximately in this example, because the exact location of the node is not known, and the lake bed rises sharply to the south of its presumed position. On a section over the sill 200 m north of station *R* the mean depth of the bottom layer would be only 11 m. The velocity in the bottom layer at this point may therefore be nearly double that shown in figure 22 and the velocity in the middle layer would be correspondingly greater.

Flow in each layer follows a pattern of alternating northerly (positive) and southerly (negative) pulses of widely differing duration. In the top layer, as would be expected from inspection of figure 10, each pulse lasts for about  $9\frac{1}{2}$  h, but the amplitudes show a slow variation resulting from interference by the third mode (41 h wave). Being least in thickness, the highest velocities are encountered in the top layer, where a peak value of 6 cm/s is reached (i.e. allowing for damping; 7.8 cm/s with no damping). In the bottom layer, which is also the thickest, velocities are less than in the other two layers. Flow in the bottom layer is complex, the result of interaction of both modes. After the first 12 h, the flow pattern consists of two short northerly pulses, alternating with slower southerly drifts of longer duration. Curiously enough, interference between the two modes is less marked in the middle layer. This follows from the  $\beta$  calculations which show that deflexions due to the 19 h mode are in phase on both interfaces and therefore partially cancel in their influence on middle-layer flow. On the other hand, deflexions on the two interfaces due to the 41 h wave are out of phase, and are therefore additive in their effect on flow in the

middle layer. Flow in this layer takes the form of long, fairly regular, alternating pulses of roughly 20 h duration. The peak velocities during the second two-thirds of the interval reviewed in figure 22 are similar in magnitude to those in the top layer.

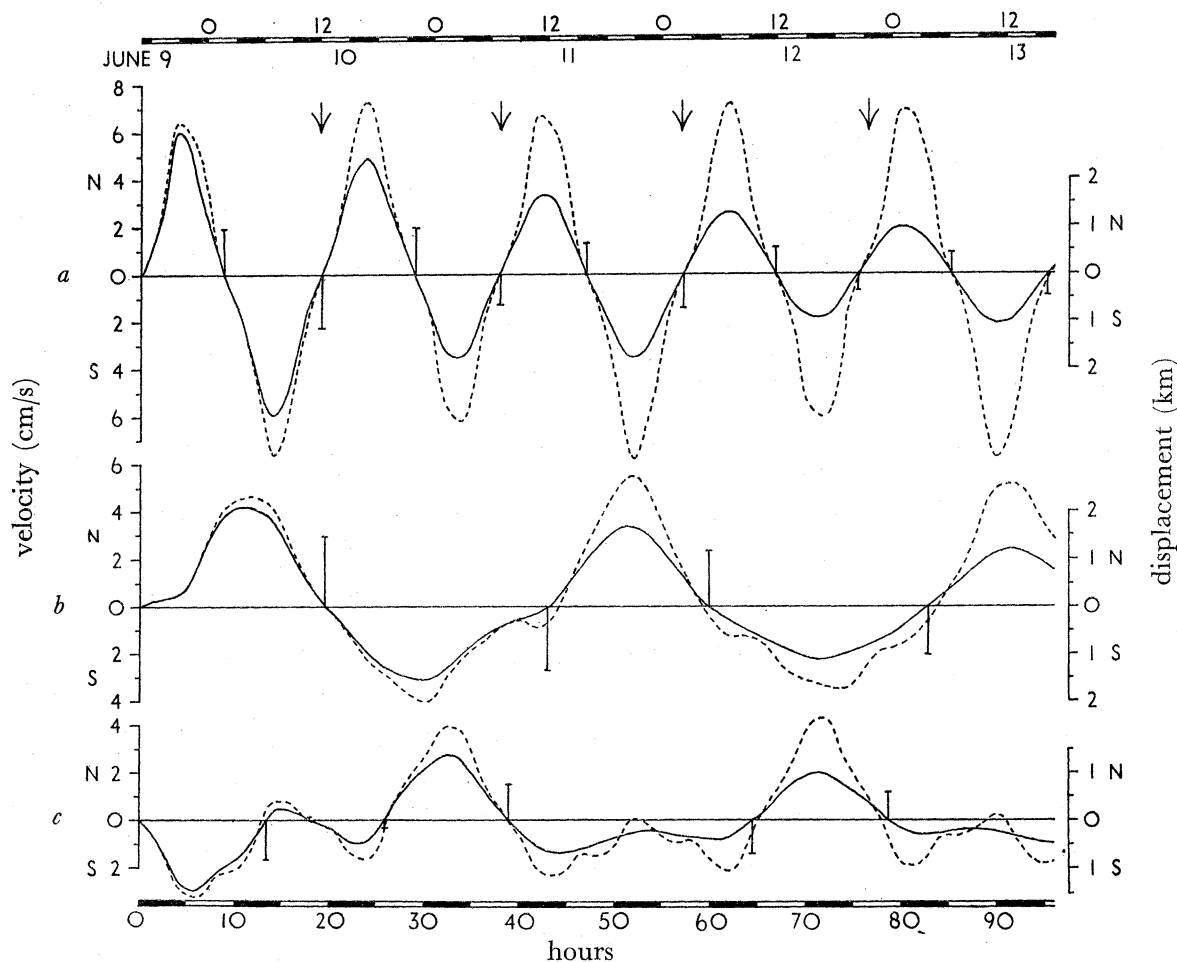


FIGURE 22. Theoretical horizontal components of velocity and displacement in (a) top, (b) middle and (c) bottom layers at the uninode of Windermere northern basin, during the interval covered by figure 19. Mean displacements due to each up-lake (N) or down-lake (S) pulse are shown as vertical lines. Velocities are shown either by dotted lines (uncorrected for damping) or unbroken lines (applying the same damping corrections as in figure 19). The arrows occupy the same points in time (presumed crests of the 19 h wave at thermocline level) as those in figure 10.

The mean horizontal displacement of a particle in each layer at the node, resulting from each northerly and southerly pulse, has been determined by planimetry and is indicated by the height of the line erected at the end of the respective pulse. This displacement bears, of course, only a general relation to the path of any particular particle or solute molecule or micro-organism in a turbulent medium. Displacements of the order of 700 m are the rule in the top and bottom layers, but the displacements in the middle layer are considerably greater, because in this layer relatively high velocities are combined with pulses of long duration. The first pulse in the middle layer corresponds to a northward displacement of 1500 m.

The picture presented in figure 22 can of course only be checked by flow measurements, but a rough check on whether or not the calculated velocities are reasonable can be made by using Taylor's (1931 *a, b*) and Goldstein's (1931) criteria of the stability of waves in various simplified cases of fluids in which both density and velocity gradients exist. The case best fitted to conditions at the thermocline appears to be one of those considered by Goldstein (1931) in which a layer of constant density and velocity and of infinite extent upwards lies above another layer of constant but different velocity, of constant but higher density, and of infinite extent downwards. These two layers are separated by a transitional layer of thickness  $h$ , in which the velocity gradient is uniform and equal to  $\alpha$  and the density gradient is equal to  $\beta\rho$ .\* If the change in density is a small fraction of the mean density then all waves which are long compared with  $h$  are stable if  $\alpha^2 < 4g\beta$ . From figure 15 we may insert approximate values:  $h = 4$  m,  $\beta = 1 \times 10^{-6}$ . Then the instability limit would be reached with a velocity difference across  $h$  of 25 cm/s. If  $\beta$  is left unchanged but  $h$  reduced to 1 m, i.e. a condition comparable with the steepest gradient shown in figure 18, the limiting velocity difference becomes 12 cm/s. Now this is not much greater than the calculated peak velocity difference between the upper and middle layers in figure 22, namely, 9.5 cm/s at about 07.00 h on 10 June. We conclude that waves of the computed magnitude would be stable at the thermocline, but that at the time of the peak velocity difference conditions may have been near the instability limit.

Conditions near the 6.7° isotherm are not so simple, as there is neither a well-marked interface nor a uniform density gradient. The best approximation available is the case considered by Taylor (1931 *a*) of a fluid extending infinitely downwards with a uniform velocity gradient  $\alpha$  and density increasing downwards at a rate  $\beta\rho$ . The stability condition for long waves is the same as in the case considered above, namely,  $\alpha^2 < 4g\beta$ . If  $\beta$  at the 20 m level (figure 15) is taken as  $0.5 \times 10^{-7}$ , then the velocity gradient above which no waves can exist is  $1.4 \times 10^{-2}$ . If we suppose that a transition layer again of the order of 4 m thickness existed between the middle and bottom layers, and that the velocity gradient was extended uniformly across it, no waves could exist if the velocity difference between layers was in excess of 5.6 cm/s. This is very near the calculated peak difference at midnight 10 to 11 June. In spite of the roughness of this test it appears that the computed waves in the lower isotherms could also have been stable, but that, as at the thermocline, the instability limit was probably very nearly reached at the time of peak velocity difference. These results suggest that, after a large wind disturbance, the density gradients may become automatically adjusted to just satisfy the stability condition for the peak velocity gradients produced by the internal waves, but these speculations can only be tested by direct observation of  $\alpha$ .

The stability calculations appear to say little about the possibility or otherwise of smaller scale turbulent motion at any level. Taylor (1931 *b*) found, after analysis of Jacobsen's data, that turbulence persisted at values of  $\alpha^2/g\beta$  of much less than unity, and there is no reason to suppose that the motion depicted in figure 22 was not turbulent at all levels. This is in agreement with the eddy diffusion coefficients calculated for the bottom waters of various lakes from the diffusion of dissolved salts and heat (Mortimer 1941, 1942).

\* It is considered desirable to retain Taylor's notation, in spite of possible confusion with the  $\beta$  of preceding paragraphs.



*Complicating factors in a lake*

The example chosen for analysis in preceding sections was a relatively simple one. Of the factors which add to the complexity of motion in a lake, multinodal seiches have been mentioned already. Others would include transverse seiches and bay seiches, the presence of progressive internal waves, the effect of friction and the effect of the earth's rotation. The last is only likely to be of significance in large lakes and will not be discussed here. In addition, there is the complexity of the energy input, namely, variations in the force and direction of the wind.

Evidence sufficiently detailed to confirm the presence of progressive internal waves in lakes does not as yet exist, but they occur in the sea (see Sverdrup, Johnson & Fleming 1942, pp. 585–602). They may be of so short a period that they have so far escaped detection, but their presence should be anticipated. It is possible that the oscillations of about 2 h period, so obvious in figure 10, can be so interpreted, although they could also be transverse seiches. However, in the light of the evidence adduced during the discussion on damping, it seems unlikely that transverse seiches could be so persistent.

As far as the seiche period is concerned, damping alone should have little effect on the period, although it may influence it through the redistribution of density achieved by mixing. As seiche energy is dissipated by turbulence, a comparison of the amplitude decrements of seiches, undisturbed by wind, may throw useful light on the variation of turbulence with lake dimensions and density distribution. At present it is impossible to say how much of the friction should be assigned to the sides and bottom and how much to the interfaces across which velocity gradients occur. In spite of the large velocity gradients across it, the thermocline may not be the main seat of friction, for high stability suppresses turbulence and enables this interface to function as the main plane of slip. The combined effect of various operative factors is complex, but in general any decrease in velocity gradient or increase in density gradient across the interface will decrease the damping of the seiche. With a deeper epilimnion and often a sharper thermocline in autumn than earlier in the year, there may therefore be a tendency for seiche damping to decrease as the season of thermal stratification advances, although so far there is no evidence to support this.

Of the reaction of a lake to the complexity of wind impulses little can be said. Johnson's (1946, 1948) experiments and observations on this subject are worthy of careful study. Examples of both the damping and the forcing of existing oscillations by wind are illustrated in figure 12, and several such were noted by Wedderburn (1912). Figure 12 also illustrates the predominance of the longitudinal uninodal seiche. It appears that, subjected to variable wind forces, a stratified lake will resonate with those periodicities in the wind 'spectrum' which correspond to uni- or sometimes multinodal seiches along the main axes. If damping is least (per unit time) for the uninodal seiche, it is not surprising that it predominates with occasional phase shifts forced by changes of wind. It is not, however, impossible that when wind action is confined to a portion of a lake, or when its shape is complex, a multinodal seiche may dominate, but no example has hitherto been observed.

*The influence of internal waves on lake biology and sedimentation*

The effect of water movements, of the magnitudes calculated in earlier sections, on mixing and on the transport of nutrient substances should be sufficiently clear without

further emphasis. In particular, the hypolimnion cannot, as so often in the past, be regarded as a stagnant layer. Turbulence may indeed be greater in the hypolimnion than in the thermocline region in spite of the large velocity gradients existing there. The influence of internal waves on the distribution of plankton, fish, etc., has yet to be investigated, but it may sometimes be considerable. If, before the wind disturbance, there is a marked vertical zonation of plankton associated with density distribution, then during wind displacement and the following internal waves the composition of vertical hauls at stations distant from the nodes will change with changing proportions of the various layers in the water column (cf. figure 10). Demoll (1921) pointed out that 'plankton waves' may be expected where 'temperature waves' are in progress. The movements of actively migrating zooplankton may, of course, largely overcome vertical displacement due to internal waves, but it is doubtful if this compensation is always complete. Möller (1928) also discusses the effect of internal waves on plankton distribution, and it is clear that any study of vertical distribution or migration of plankton which aims to be quantitative must take such movement into account.

Phytoplankton, on the other hand, must, with few exceptions, drift with the surrounding water, and large changes in vertical distribution due to internal waves are to be expected at stations distant from the node, especially where peak numbers occur in the metalimnion. In actual examples it may often be difficult, without knowledge of previous dynamic history, to distinguish movement due to direct wind action and that due to internal waves. Although such a distinction may be of value in theoretical analyses, when considering biological effects it is usually more convenient to regard the two phases as part of one whole, the reaction of a stratified lake to wind. Although they refer to the wind-displacement phase only, the results of Thomas (1949) are of interest in this connexion. He records a thermocline tilt in the Zürichsee which was accompanied by a similar tilt of the layer containing the maximum numbers of *Oscillatoria rubescens*, and an even more remarkable case (Thomas 1950) in the same lake, in which the thermocline tilt had been maintained for several days by continued winds, but in which the 'Oscillatoria layer' had reverted to a horizontal position. This last result, which Thomas attributes to a phototropic reaction, would repay examination in more detail. Flück (1927) also noted the effect of wind in bringing plankton from deeper layers to the surface at the windward end of the Brienersee.

The dynamics of sedimentation of plankton and other particles will be profoundly influenced by internal waves and the associated turbulence. For phytoplankton cells, which possess no means of active movement, the scale of turbulent mixing is especially important, as it determines what proportion of its life a cell may expect to spend in illuminated surface waters. In a well-stirred epilimnion the cells may expect to remain in suspension a relatively long time. But some will get into the thermocline and sink faster in this region of high stability and low turbulence. Once through this layer they enter another medium in which turbulence may at times be higher than in the one they have just left. They may remain suspended for a while, but their chances of being returned to the epilimnion are very small. Eventually they will be carried, or sink, to the bottom, and it may be supposed that movement in the hypolimnion will have considerable influence on their actual deposition. Deposition will occur more readily whenever and wherever flow,

and the turbulence associated with it, falls to zero (i.e. at the antinodes). On the other hand, turbulence will be most intense at the nodes, and internal waves of large amplitude may even cause resuspension of the finer particles in nodal regions. Munk (1941) describes a multinodal standing wave in the Gulf of California, apparently maintained by resonance with the lunar fortnightly tidal period. The maximum velocity at the nodes was as high as 20 cm/s. Munk points out that Revelle (1939) found the distribution of particle size of bottom sediments to vary, along a longitudinal section, in a regular manner corresponding to a trinodal internal wave. The largest average diameters were found at the nodes.

#### SUMMARY

The first part of this paper is taken up with an historical survey of the relatively few observations, some detailed and some less so, of internal seiches (internal standing waves) in lakes. After a description of the thermo-electric thermometer employed (figure 2), there follow details and illustrations of the evidence, from temperature observations, for such internal waves in the northern basin of Windermere. Two main phases could be distinguished: (i) motion under wind stress leading to quasi-steady states with some or all of the isotherms tilted (cf. figures 5, 8 and 21); (ii) internal seiche motion which developed after the wind had dropped (figures 10, 12). These observations confirm the findings of Wedderburn and his collaborators on the Scottish Lochs (1907–15). The results from Windermere are presented, not because any such confirmation is necessary, but in order to secure belated recognition of the fact that Wedderburn's 'temperature seiche' is not an isolated phenomenon, but is an everyday feature of movement in stratified lakes subject to wind action. As this movement is an important and largely unrecognized factor in lake environment, this paper is addressed mainly to limnologists. In its latter part, results of theoretical analyses of a detailed series of observations (figures 8, 10) are presented in non-mathematical form. The applicability of a theory of oscillations in a basin with three layers of differing density (set out in an appendix by M. S. Longuet-Higgins) is tested by comparing (in figure 19) theoretical and observed deflexions of selected isotherms from their equilibrium levels, resulting from internal waves after a gale. This theory also enables horizontal components of velocity and displacement to be calculated for each layer (figure 22). Complicating factors in natural lakes are enumerated, and the influence of internal waves on lake biology and sedimentation is discussed.

During motion under wind stress the isotherms nearer the surface were generally tilted more steeply than those at lower levels. Under steady wind conditions, the isotherms formed a fan with the 'handle' (i.e. a sharp thermocline) at the leeward end of the basin (compare figures 8, 21 *b* and model experiments, figure 14 *a, b*). To produce this distribution, water at intermediate levels had been shifted to windward. With strong winds the shift was great enough to force this intermediate water (and, in extreme cases, bottom water) to the surface at the windward end (table 1, figure 8 *a* and model experiments, figure 14 *c, d*). When this occurred, water from middle and lower layers became caught up in the surface wind-drift and was mixed into the epilimnion. This mechanism explains the deepening of the epilimnion and the steepening of the thermocline gradient, often noted in lakes after windy spells.

These displacements were resolved, when the wind stopped, into internal waves at various levels. In a number of examples the most obvious feature was, as Wedderburn found, a uninodal longitudinal internal seiche at thermocline level with a period in Windermere of 15 to 20 h. This seiche, which may be regarded as the main 'resonance' of the basin, was set in motion by quite moderate winds, but was continually modified by transverse seiches (figure 7) and by changes of amplitude and phase forced by new wind impulses (figure 12).

In one example (figure 10) hourly measurements at one station during 3 days following a gale showed, not only a regular wave of 19 h period and 2 to 3 m amplitude at thermocline level, but also movement of complex wave-form, longer period and greater amplitude at lower levels. The first result can be predicted (table 2) by the well-known theory of standing waves in a basin with two fluid layers (first applied to a lake by Watson 1904), but this theory provides no information on waves which may be set up at lower levels.

It is clear that complete interpretation of these movements must await a more general theory of oscillations in a basin in which density varies continuously with depth, as in the lake. Nevertheless, a helpful *interim* step is the interpretation of the waves observed in figure 10 as oscillations in a basin containing *three* layers, the dimensions and densities of which have been fitted to lake conditions (figure 15). The wind effects, noted earlier, can be interpreted in terms of such a three-layered model (compare figures 8, 21 and 14), and the theory given in the appendix is able to predict subsequent deflexions of the two internal interfaces, if their initial displacements from equilibrium are known. These deflexions result from a combination of two internal modes of oscillation (neglecting the surface seiche), whose periods are given by equations (5) and (6), while the ratio of the amplitude which appears on one interface to that which appears on the other is given, for each mode, by equation (8). If the density difference at one interface is considerably different from that at the other, the periods of the modes will also differ widely. The effect on the period calculation of small variations in choice of dimensions and densities of the layers in a model fitted to lake conditions is demonstrated in table 2. In any particular example the initial amplitudes of each mode, as well as the number and amplitude of the harmonics which may be excited, depends on the previous history of the wind disturbance. Knowledge of which harmonics are important in any particular case, and their appropriate coefficients for insertion in the deflexion equations (A17), are derived from a Fourier analysis of the initial displacements of the interfaces.

Selecting the 11° and 6·7° isotherms to represent, respectively, the upper and lower interfaces, and assuming that their displacement at the end of the gale (figure 8*b*) depicts a state of rest from which the oscillations started, subsequent isotherm deflexions were calculated and compared, in figure 19, with those observed. The observed deflexions (figure 10) were clearly subject to damping, but as the theory takes no account of this (figure 19*a*), an estimated damping coefficient equivalent to 23 % amplitude decrease *per cycle* (or a log decrement of 0·26) was applied equally to both modes and to each of their harmonics, in order to achieve a reasonable fit between theory and observation (figure 19*b*). If damping in nature also followed this plan, and the agreement in figure 19*b* suggests that it did, the higher harmonics produced by the gale were damped out more rapidly (per unit time)

than the fundamental modes. This result can be illustrated in model experiments (figure 20), and it would explain the persistence of the uninodal internal seiche as a 'resonant' response of the stratified lake to wind (figure 12).

In figure 19 the deflexion of the  $11^{\circ}$  isotherm appears to be mainly controlled by one mode, and is a close fit to the observed internal seiche of about 19 h period at thermocline level. This, of course, is no more than was predicted by the two-layer theory. The novel result of the three-layer theory lies in the disclosure of another mode of 40 to 50 h period, which in combination with the 19 h mode reproduces in all major particulars the observed variation in level of the  $6.7^{\circ}$  isotherm. This result appears the more remarkable when the discrepancies between lake conditions and the hypothetical model are examined. For, although the homogeneous top and bottom layers in the model can be fitted to more or less homogeneous layers in the lake, the homogeneous middle layer in the model finds no counterpart in nature. The influence of the 40 to 50 h. mode is also seen (dotted line in figure 19*b*) as a long-period shift in the general level of the thermocline oscillation.

A more useful application of this theory for the hydrobiologist is the calculation of the horizontal components of velocity and displacement in each layer. This has been done for the above numerical example at the uninode; the results are presented in figure 22. Movement in the top and bottom layers is probably not widely different from that which occurred in the lake during the interval covered by figure 10, but the velocity distribution in the middle layer was certainly more complex in the lake than that indicated in figure 22. Flow in each layer took the form of alternating pulses up (N) and down (S) the lake. Maximum velocities, after applying the same arbitrary damping factor as in figure 19, were 6 cm/s in the top layer, 4 cm/s in the middle and 3 cm/s in the bottom layer, while equivalent mean horizontal displacements were 1, 1.5 and 0.7 km. As might be expected, velocity and displacement are least in the bottom layer. Nevertheless, there is ample movement to account for the intensity of turbulence estimated (Mortimer 1941, 1942) from the diffusion of various properties near the bottom of various lakes. This picture of flow, subject though it is to the confirmation of measurement, shows how it comes about that stratified lakes with high stability, with little mixing between the layers, and with what in the past have usually been taken to be signs of stagnation (e.g. oxygen depletion) in the bottom layers, can nevertheless show undoubted evidence of large-scale horizontal movement at all levels.

My indebtedness to M. S. Longuet-Higgins for setting out the theory in the appendix and for sorely needed guidance with the mathematics has already been expressed. In addition to the help already noted in connexion with table 1, I am glad to acknowledge the assistance of other colleagues without whose help this work would not have been completed. I am particularly indebted to W. H. Moore for construction of the thermo-electric thermometer and for a large part of the measurements, also to F. J. Mackereth for observations during the night of 11 June 1947, to A. E. Ramsbottom for computation and preparation of figures and to H. C. Gilson, Dr J. W. G. Lund and Dr L. H. N. Cooper for criticizing the manuscript.

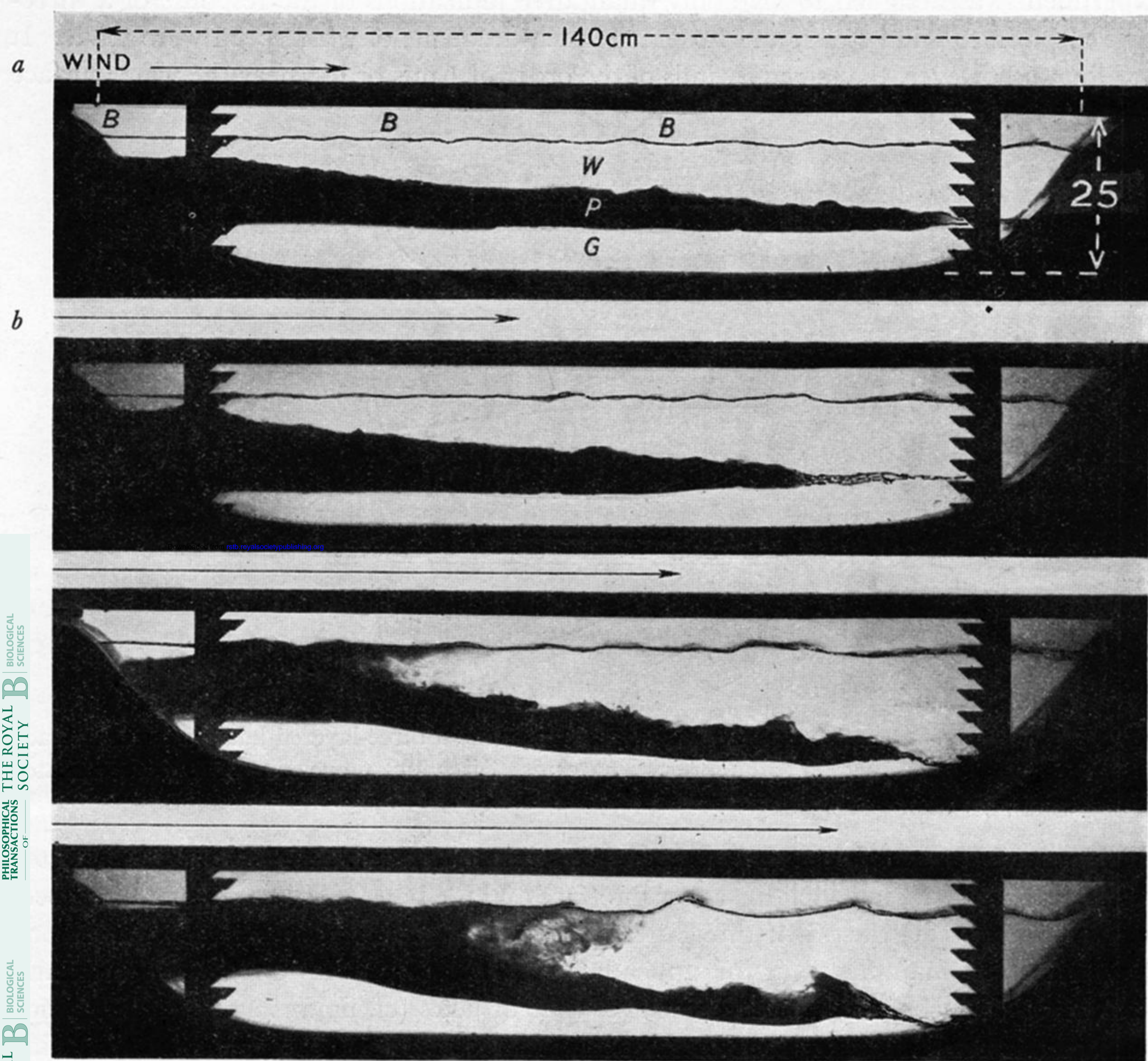


FIGURE 14. The effect of wind stress on a model lake containing three layers of differing density. Wind force is indicated roughly by the length of the arrows; (*a*) and (*b*) steady moderate winds, (*c*) and (*d*) more violent winds. Blowers were situated at *B*. The fluids used, and their approximate densities, were: water (*W*) 1.00, commercial cresol (*P*) 1.04 and 25 % glycerine solution (*G*) 1.06.

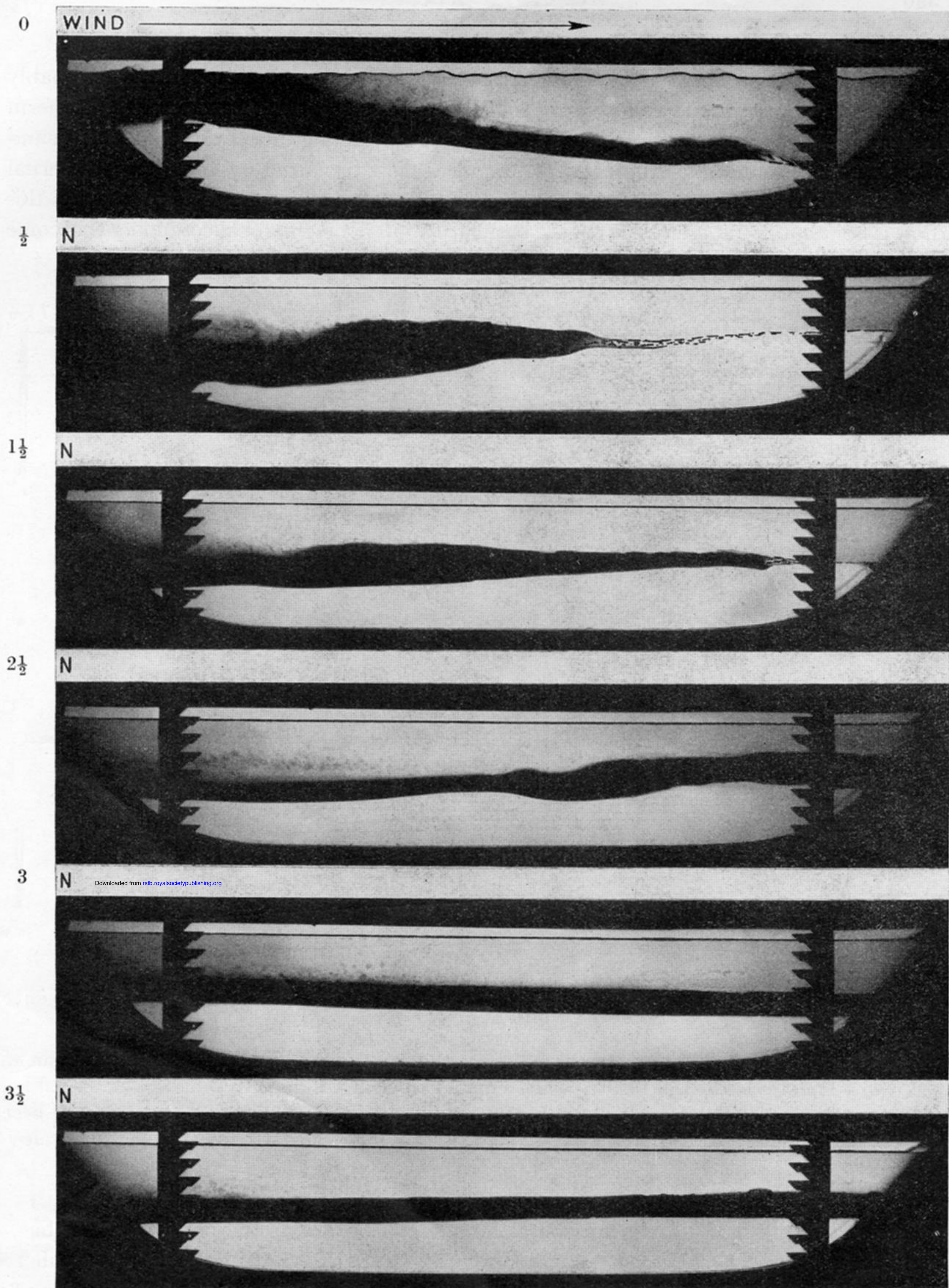


FIGURE 20. Internal waves, after wind stress, in a model lake with three layers of differing density (for details of the layers see figure 14). The initial condition under wind stress is shown in the top picture; the lower pictures (N=no wind) illustrate successive stages in the oscillations which followed after the wind had stopped. The number of cycles through which the main oscillation had passed are given on the left of the figures.